HAL
open science

One-sided Adaptive Truncated Exponentially Weighted Moving Average X Schemes for Detecting Process Mean Shifts

Fupeng Xie, Philippe Castagliola, Zhonghua Li, Jinsheng Sun, Xuelong Hu

To cite this version:

Fupeng Xie, Philippe Castagliola, Zhonghua Li, Jinsheng Sun, Xuelong Hu. One-sided Adaptive Truncated Exponentially Weighted Moving Average X Schemes for Detecting Process Mean Shifts. Quality technology & quantitative management, 2022, 19 (5), pp.533-561. 10.1080/16843703.2022.2033404 . hal-03764697

HAL Id: hal-03764697

https://hal.science/hal-03764697v1

Submitted on 30 Aug 2022

HAL is a multi-disciplinary open access archive for the deposit and dissemination of scientific research documents, whether they are published or not. The documents may come from teaching and research institutions in France or abroad, or from public or private research centers.

L'archive ouverte pluridisciplinaire **HAL**, est destinée au dépôt et à la diffusion de documents scientifiques de niveau recherche, publiés ou non, émanant des établissements d'enseignement et de recherche français ou étrangers, des laboratoires publics ou privés.

One-sided Adaptive Truncated Exponentially Weighted Moving Average $\bar{X}$ Schemes for Detecting Process Mean Shifts

FuPeng Xie [1], Philippe Castagliola[2], Zhonghua Li[3], JinSheng Sun[1] and XueLong Hu [*4]

[1]*School of Automation, Nanjing University of Science and Technology, Nanjing, China*

[2]*Université de Nantes & LS2N UMR CNRS 6004, Nantes, France*

[3]*School of Statistics and Data Science and LPMC and KLMDASR, Nankai University, Tianjin, China*

[4]*School of Management & Institute of High-Quality Development Evaluation, Nanjing University of Posts and Telecommunications, Nanjing, China*

Abstract

One-sided type schemes are known to be more appropriate for monitoring a process when the direction of a potential mean shift can be anticipated. Furthermore, if the magnitude of the potential mean shift is unknown, it is desired to design a control chart to perform well over a wide range of shifts instead of only optimizing its performance in monitoring a particular mean shift level. The one-sided adaptive truncated exponentially weighted moving average (ATEWMA) $\bar{X}$ scheme recommended in this paper is a control chart that combines a Shewhart $\bar{X}$ scheme and a new one-sided EWMA $\bar{X}$ scheme together in a smooth way for rapidly detecting the upward (or downward) mean shifts. The basic idea of the recommended one-sided ATEWMA $\bar{X}$ scheme is to truncate the observations (i.e., the sample means $\bar{X}$) first, and then to dynamically weight the past observations according to a suitable function of the current prediction error. This helps to improve the sensitivity of the proposed one-sided ATEWMA $\bar{X}$ scheme for detecting both small and

*Corresponding Author: XueLong Hu. Email: hxl0419@hotmail.com

large mean shifts simultaneously. In addition, to further improve the detection efficiency of the recommended scheme, we also suggest integrating a variable sampling interval (VSI) feature into the proposed one-sided ATEWMA $\bar{X}$ scheme. Markov chain models are established to analyze the run length (RL) properties of the recommended one-sided ATEWMA $\bar{X}$ scheme in both the zero-state and the steady-state cases. Comparison results show that the recommended one-sided ATEWMA $\bar{X}$ scheme works better than the conventional adaptive EWMA (AEWMA) $\bar{X}$ chart and the improved one-sided EWMA $\bar{X}$ chart in detecting a wide range of mean shifts. Finally, a numerical example is presented to illustrate the usage of the proposed one-sided ATEWMA $\bar{X}$ scheme for detecting process mean shifts.

Keywords: Adaptive EWMA $\bar{X}$ control chart; Markov chain model; One-sided type scheme; Truncation method; Variable sampling interval;

1 Introduction

As one of the most important tools in statistical process monitoring (SPM), control charts have been extensively used in various fields to monitor possible deteriorations of processes, for instance, chemical and process industries, natural disaster monitoring, or healthcare. Readers can refer to Anwar et al. (2020), Perry (2020), Zhou et al. (2020), and Chong et al. (2020) for some recent research works on the application of control charts. Among the traditional control charts, Shewhart-type ones received much attention because they are easy to implement and very effective for monitoring large shifts. On the other hand, memory-type charts (for instance, the exponentially weighted moving average (EWMA) and the cumulative sum (CUSUM) charts), which take into account the past information from the beginning to the most current state of the process, can be regarded as good alternatives to the Shewhart-type schemes in monitoring small to moderate shifts (see Castagliola et al. (2019) and Hu et al. (2019)). For more details about these traditional control charts, readers can refer to Montgomery (2012).

According to Haq & Khoo (2020), shift sizes in real applications are commonly unknown *a priori*, and they must be estimated in advance or expected to belong to a certain shift range. In general, most

of traditional control charts are designed for monitoring a particular shift level only, which leads to the fact that these traditional schemes can hardly provide an effective way for detecting both small and large shifts simultaneously. For example, a standard EWMA chart with a small smoothing parameter is more effective for detecting small shifts of the process, while a large smoothing parameter of this scheme can provide more protection against large shifts, see Tang et al. (2019a). In this context, an adaptive EWMA (AEWMA) chart in Capizzi & Masarotto (2003) was designed to give a balanced protection against a range of mean shifts. Different from the traditional standard EWMA chart, the charting statistic Q_t of the conventional AEWMA chart is defined as,

$$Q_t = \omega(e_t)X_t + (1 - \omega(e_t))\, Q_{t-1},$$

where $\{X_1, X_2, \cdots, X_t\}$ is a i.i.d. (independent and identically distributed) sequence of normal random variables with mean μ_0 and standard deviation σ_0. Additionally, the weighted parameter $\omega(e_t)$ is defined as $\phi(e_t)/e_t$, where $\phi(e_t)$ denotes a score function and $e_t = X_t - Q_{t-1}$ is the prediction error. Since a suitable function of the current error e_t is used to weight the past and current observations, the conventional AEWMA chart can be viewed as a smooth combination of a Shewhart chart and an EWMA chart. As pointed out by Psarakis (2015), many research works have been done on adaptive type schemes, especially for adaptive EWMA charts. For example, Shu (2008) extended the basic idea of the AEWMA scheme in detecting process locations to the case of monitoring process dispersion. Su et al. (2011) analyzed the performance of AEWMA schemes in detecting linear drifts of process mean, and Tang et al. (2019c) investigated both the median run length (MRL) and the expected median run length (EMRL) performance of the AEWMA $\bar{X}$ scheme for the zero-state and the steady-state. In addition, Tang et al. (2019d) proposed a new nonparametric AEWMA type scheme with exact run length (RL) properties, which combines the advantages of a nonparametric chart with the better overall shift detection capability of the AEWMA scheme. All of these research works show that AEWMA type schemes have wide potential applications in the future.

In practice, there are many situations where only upward or downward shifts need to be detected. For instance, an increase in the infection rate of a particular disease (such as the COVID-19) indicates an increased risk to the public health, and the corresponding information is very important for local

governments to adjust epidemic prevention and take measures to the public. It has been shown that a one-sided type scheme is more appropriate for process monitoring, if the direction information of potential shifts can be anticipated. In this paper, two commonly used one-sided EWMA type charts are introduced. The one-sided EWMA chart with reflecting boundaries (hereafter denoted as the one-sided REWMA chart) was first developed by Champ et al. (1991), the basic idea of this scheme is to reset the standard EWMA charting statistic to the value of the reflecting boundary whenever it is below (or above) the reflecting boundary for the upper-sided (or the lower-sided) REWMA chart. The corresponding upper- and lower-sided REWMA charting statistics can be defined as follow s,

$$Q_{R,t}^{+} = \max\left(B_U, r'X_t + (1-r')Q_{R,t-1}^{+}\right),$$
$$Q_{R,t}^{-} = \min\left(B_L, r'X_t + (1-r')Q_{R,t-1}^{-}\right),$$

where B_U (or B_L) represents the upper-sided (lower-sided) reflecting boundary of the upper-sided (lower-sided) REWMA scheme, and $r' \in (0,1]$ is the smoothing factor of the one-sided REWMA scheme. Up to now, this type of scheme has been adopted by many researchers. For instance, Gan (1998) developed one- and two-sided exponential EWMA charts with reflecting boundaries for monitoring the rate of occurrences of rare events. Zhang & Chen (2004) designed a one-sided EWMA chart with reflecting boundaries to monitor the mean of censored Weibull lifetimes. Different from the one-sided REWMA charts, Shu et al. (2007) proposed a new improved one-sided EWMA chart using a truncation method (denoted as the one-sided TEWMA chart hereafter) for normally distributed data. The idea of this scheme is to truncate the negative (or positive) deviations from the target to zero, and to only accumulate the positive (or negative) deviations from the target in the computation of the EWMA statistic at each timestep. The charting statistics of the upper- and lower-sided TEWMA charts are,

$$Q_{T,t}^{+} = rX_t^{+} + (1-r)Q_{T,t-1}^{+},$$
$$Q_{T,t}^{-} = rX_t^{-} + (1-r)Q_{T,t-1}^{-},$$

where $X_t^+ = \max(\mu_0, X_t) = \mu_0 + \max(0, X_t - \mu_0)$, and $X_t^- = \min(\mu_0, X_t) = \mu_0 + \min(0, X_t - \mu_0)$. Also, $r \in (0, 1]$ represents the smoothing factor of the one-sided TEWMA scheme. Numerical results in Shu et al. (2007) have shown that the one-sided TEWMA scheme performs better than both the standard EWMA chart and the one-sided REWMA scheme for detecting mean shifts in terms of zero-state, steady-state, and worst-case scenarios. Motivated by the new "resetting rule" used in the one-sided TEWMA scheme, Shu & Jiang (2008) proposed a new EWMA dispersion chart by truncating negative normalized observations to zero in the traditional EWMA statistic. Shu et al. (2012) extended the truncation method to Poisson processes using a normalizing transformation. Furthermore, Haq (2020) constructed one-sided and two one-sided multivariate EWMA chart s using the truncation method for monitoring mean vectors of multivariate normal process es.

A common practice of using a control chart for process monitoring is to take a fixed sample size from the process with a fixed sampling interval (FSI). Extensive research works have shown that varying the sampling interval as a function of the observation can make the shift detection faster than its corresponding FSI strategy, see Saccucci et al. (1992), Reynolds Jr & Arnold (2001), and Haq (2019). In general, two sampling intervals (i.e., a short sampling interval d_S and a long sampling interval d_L) are sufficient for variable sampling interval (VSI) type schemes to provide good performance in different shift detections (see Reynolds et al. (1988) and Reynolds Jr (1989)). The basic idea of the VSI type scheme is that the short sampling interval d_S will be taken to ensure a quick shift detection when a possible out-of-control situation is indicated, and the long sampling interval d_L will keep being used if there is no suspected process shift. Note that the short sampling interval d_S is usually selected in the zero-state case as a safeguard to provide additional protection against possible shifts that occur upon startup, i.e., $d_0 = d_S$, where d_0 is the initial sampling interval. More recently, Liu et al. (2015) proposed an adaptive Phase II nonparametric EWMA chart with a VSI feature. Tang et al. (2017) studied the effects of the VSI feature on the AEWMA $\bar{X}$ scheme, and then further analyzed the selection of two sampling intervals based on the average time to signal (ATS) and the adjusted steady-state ATS (AATS). In addition, Haq et al. (2021) investigated the RL characteristics of the adaptive CUSUM and EWMA schemes with auxiliary information and VSI strategy.

Motivated by the fact that, (1) compared with the standard EWMA scheme and the one-sided REWMA scheme, the truncation method used in the one-sided TEWMA chart can significantly improve the sensitivity of the scheme in detecting either increase or decrease in the process mean, and (2) the AEWMA scheme can provide better overall protection against different mean shifts than the standard EWMA scheme, the purpose of this paper is to develop a new one-sided type scheme, which combines the advantages of "adaptive" and "truncated", to perform well for both small and large shifts assuming a known shift direction. Furthermore, it is known that the VSI feature can notably improve the performance of control charts in terms of the ATS. Therefore, we also suggest integrating a VSI feature into the proposed one-sided type scheme to investigate its zero- and steady-state ATS performance. To sum up, the key contributions of this paper are as follows:

- To propose a new one-sided AEWMA $\bar{X}$ type scheme using a truncation method (hereafter named as the one-sided ATEWMA $\bar{X}$ scheme), and then to establish a dedicated Markov chain model for evaluating the RL properties of the proposed one-sided ATEWMA $\bar{X}$ scheme in both the zero-state and the steady-state cases.

- To integrate a VSI feature into the proposed one-sided ATEWMA $\bar{X}$ scheme (hereafter denoted as the one-sided VSI-ATEWMA $\bar{X}$ scheme) to improve its detection efficiency in monitoring upward or downward shifts of the process mean.

- To develope an optimal design procedure of the proposed one-sided ATEWMA $\bar{X}$ scheme for monitoring both small and large mean shifts simultaneously.

The outline of this paper is given as follow s: In Section 2, a new one-sided ATEWMA $\bar{X}$ scheme using a truncation method is first introduced. In Section 3, a dedicated Markov chain model is established to investigate the RL properties of the recommended one-sided ATEWMA $\bar{X}$ scheme in both the zero-state and the steady-state cases. Furthermore, an optimal design procedure of the recommended one-sided ATEWMA $\bar{X}$ scheme is developed for monitoring both small and large shifts simultaneously. A discussion about how to extend the proposed one-sided ATEWMA $\bar{X}$ scheme to its VSI counterpart is introduced in detail in Section 4. Subsequently, numerical comparisons are performed with the conventional AEWMA $\bar{X}$ chart and the one-sided TEWMA $\bar{X}$ chart in term s of upward mean shift detection. Several guidelines for constructing the proposed one-sided ATEWMA

$\bar{X}$ scheme and its VSI counterpart are also provided in Section 5. In Section 6, a simulated example is presented to illustrate the usage of the recommended one-sided ATEWMA $\bar{X}$ scheme for two different scenarios. Finally, Section 7 concludes with some remarks and directions for future researches.

2 Design of the one-sided ATEWMA $\bar{X}$ scheme

For the quality characteristic X to be monitored, let us assume that $\{X_{t,1}, X_{t,2}, \cdots, X_{t,n}\}$ is a sample of $n \geqslant 1$ independent normal random variables taken at regular sampling point $t = 1, 2, 3, \cdots$. More specifically, $X_{t,i} \sim N(\mu_0 + \delta\sigma_0, \sigma_0)$, where $i = 1, 2, \cdots, n$, μ_0 and σ_0 represent the known in-control mean and standard deviation, respectively, and δ is the magnitude of the standardized mean shift. The process is deemed to be in-control when $\delta = 0$. Otherwise ($\delta \neq 0$), the process is out-of-control. Furthermore, the sample means $\bar{X}_t = \frac{1}{n}\sum_{i=1}^{n} X_{t,i}$ are plotted on the control chart for the process monitoring.

For quickly detecting increases (or decreases) of the process mean, a truncation method proposed by Shu et al. (2007) is employed in the recommended one-sided ATEWMA $\bar{X}$ scheme. The basic idea of the truncation method used in this paper is to truncate the sample mean $\bar{X}$ below (or above) the in-control mean μ_0 to the value of μ_0, and to only accumulate the sample mean $\bar{X}$ above (or below) the in-control mean μ_0 in the iterative calculation of the charting statistic. Without loss of generality, the truncation method can be achieved by using the upper- and lower-truncated random variables defined as follow s,

$$\bar{X}_t^+ = \max(\mu_0, \bar{X}_t), \tag{1}$$

$$\bar{X}_t^- = \min(\mu_0, \bar{X}_t). \tag{2}$$

In this paper, the definition of the standard normal random variable $Y_t = \sqrt{n}(\bar{X}_t - \mu_0)/\sigma_0$ is suggested to simplify the design of the recommended one-sided ATEWMA $\bar{X}$ scheme. Then, the upper- and lower-truncated random variables can be simply restated as,

$$Y_t^+ = \max(0, Y_t), \tag{3}$$

$$Y_t^- = \min(0, Y_t). \tag{4}$$

When the process is deemed to be in-control (i.e., $\delta = 0$), the mean and variance of the upper-truncated random variable Y_t^+ are $E(Y_t^+) = 1/\sqrt{2\pi}$ and $V(Y_t^+) = (\pi - 1)/2\pi$, respectively. Similarly, the in-control mean and variance of the lower-truncated random variable Y_t^- are $E(Y_t^-) = -1/\sqrt{2\pi}$ and $V(Y_t^-) = (\pi - 1)/2\pi$, respectively (see Barr & Sherrill (1999)). Furthermore, let us define the standardized upper- and lower-truncated random variables as follow s,

$$Z_t^+ = \frac{Y_t^+ - 1/\sqrt{2\pi}}{\sqrt{(\pi - 1)/2\pi}}, \tag{5}$$

$$Z_t^- = \frac{Y_t^- + 1/\sqrt{2\pi}}{\sqrt{(\pi - 1)/2\pi}}. \tag{6}$$

Different from the standard upper-sided (or lower-sided) TEWMA $\bar{X}$ chart with a fixed weight, the proposed upper-sided (lower-sided) ATEWMA $\bar{X}$ scheme is designed by adjusting the weighted parameter $\omega(e_t^+)$ (or $\omega(e_t^-)$) as a function of the prediction error $e_t^+ = Z_t^+ - Q_{t-1}^+$ $\left(e_t^- = Z_t^- - Q_{t-1}^-\right)$. Therefore, in the current context, the upper- and lower-sided ATEWMA charting statistics can be written as follow s,

$$Q_t^+ = Q_{t-1}^+ + \phi(e_t^+) = \omega(e_t^+) Z_t^+ + \left(1 - \omega(e_t^+)\right) Q_{t-1}^+, \tag{7}$$

$$Q_t^- = Q_{t-1}^- + \phi(e_t^-) = \omega(e_t^-) Z_t^- + \left(1 - \omega(e_t^-)\right) Q_{t-1}^-, \tag{8}$$

where Q_t^+ and Q_t^- are the upper- and lower-sided ATEWMA charting statistics obtained at the sampling point t, respectively. The initial values of Q_t^+ and Q_t^- are usually taken to be $E(Z_t^+) = E(Z_t^-) = 0$. In addition, $\omega(e_t^+) = \phi(e_t^+)/e_t^+$ and $\omega(e_t^-) = \phi(e_t^-)/e_t^-$ represent the variable weights of the upper- and lower-sided ATEWMA $\bar{X}$ scheme, where $\phi(\cdot)$ is a score function. The score function used in this paper is the Huber's score function $\phi_H(e)$ defined as,

$$\phi_H(e) = \begin{cases} e + (1-\lambda) \times k, & e < -k \\ \lambda \times e, & |e| \leqslant k \\ e - (1-\lambda) \times k, & e > k \end{cases}, \tag{9}$$

where $k \geqslant 0$, and $\lambda \in (0, 1]$ is the smoothing factor of the recommended one-sided ATEWMA $\bar{X}$ scheme. It is worth noting that when $k \to \infty$, $\phi_H(e) \approx \lambda e$, and when $k \to 0$, $\phi_H(e) \approx e$. For an upward (or downward) mean shift detection, the recommended upper-sided (lower-sided) ATEWMA $\bar{X}$ scheme will trigger an out-of-control signal if the charting statistic $Q_t^+ > H^+$ ($Q_t^- < H^-$), where $H^+(H^-)$ is the upper (lower) control limit of the upper-sided (lower-sided) ATEWMA $\bar{X}$ scheme.

3 Run length properties of the proposed scheme

By definition, the average run length (ARL) is the average number of observations required for a FSI type scheme to trigger an out-of-control signal. Generally, the RL properties of EWMA type control charts are approximated by using integral equations, Markov chain methods or Monte Carlo simulations. In this paper, a dedicated Markov chain model is established to evaluate the ARL performance of the recommended one-sided ATEWMA $\bar{X}$ schemes. Due to the space limitation, only the upper-sided ATEWMA $\bar{X}$ scheme is discussed here for illustration. For more details about the Markov chain model of the recommended lower-sided ATEWMA $\bar{X}$ scheme, readers can refer to the Appendix A. It is easy to verify that the upper-sided ATEWMA charting statistic $Q_t^+ = \omega(e_t^+)Z_t^+ + \left(1 - \omega(e_t^+)\right) Q_{t-1}^+ \geqslant \frac{-1}{\sqrt{\pi-1}}$, and then the in-control region $\left[\frac{-1}{\sqrt{\pi-1}}, H^+\right]$ can be divided into m subintervals of width $\Delta^+ = (H^+ + \frac{1}{\sqrt{\pi-1}})/m$. The charting statistic Q_t^+ is said to be in transient state j, at the sampling point t, if $v_j^+ - \frac{\Delta^+}{2} < Q_t^+ \leqslant v_j^+ + \frac{\Delta^+}{2}$, where $j = 1, 2, \cdots, m$, and $v_j^+ = \frac{-1}{\sqrt{\pi-1}} + (j - \frac{1}{2})\Delta^+$ represents the midpoint value of the jth subinterval $E_j^+ = \left[v_j^+ - \frac{\Delta^+}{2}, v_j^+ + \frac{\Delta^+}{2}\right]$. The transition probability matrix $\mathbf{P}$ of the Markov chain model is defined as,

$$\mathbf{P} = \begin{pmatrix} \mathbf{Q} & (\mathbf{I} - \mathbf{Q})\,\mathbf{1} \\ \mathbf{0}^{\mathsf{T}} & 1 \end{pmatrix}, \tag{10}$$

where $\mathbf{Q}$ denotes an $m \times m$-dimensional submatrix that contains the transition probabilities $q_{i,j}$ of the charting statistic Q_t^+ from state i to state j. In addition, $\mathbf{0}$ is an $m \times 1$ column vector of 0's, $\mathbf{1}$ is an $m \times 1$-dimensional vector of 1's, and $\mathbf{I}$ is an $m \times m$-dimensional identity matrix. The transition probabilities $q_{i,j}$ in the matrix $\mathbf{Q}$ can be computed as follow s,

$$\begin{aligned} q_{i,j} &= \Pr\left(Q_t^+ \in \text{state } j \;\middle|\; Q_{t-1}^+ \in \text{state } i\right) \\ &= \Pr\left(v_j^+ - \frac{\Delta^+}{2} < Q_t^+ \leqslant v_j^+ + \frac{\Delta^+}{2} \middle| Q_{t-1}^+ = v_i^+\right) \\ &= \Pr\left(v_j^+ - v_i^+ - \frac{\Delta^+}{2} < \phi_H(Z_t^+ - v_i^+) \leqslant v_j^+ - v_i^+ + \frac{\Delta^+}{2}\right) \end{aligned} . \tag{11}$$

According to Capizzi & Masarotto (2003) and Tang et al. (2017), the Huber's inverse function $\phi_H^{-1}(u)$ can be defined as follow s,

$$\phi_H^{-1}(u) = \begin{cases} u - (1-\lambda) \times k, & u < -\lambda k \\ u/\lambda, & |u| \leqslant \lambda k \\ u + (1-\lambda) \times k, & u > \lambda k \end{cases} . \tag{12}$$

Furthermore, the transition probabilities $q_{i,j}$ are written as follow s,

$$\begin{aligned} q_{i,j} &= \Pr\left(v_i^+ + \phi_H^{-1}\left(v_j^+ - v_i^+ - \frac{\Delta^+}{2}\right) < Z_t^+ \leqslant v_i^+ + \phi_H^{-1}\left(v_j^+ - v_i^+ + \frac{\Delta^+}{2}\right)\right) \\ &= \Pr\left(E(Y_t^+) + \sqrt{V(Y_t^+)}\left[v_i^+ + \phi_H^{-1}\left(v_j^+ - v_i^+ - \frac{\Delta^+}{2}\right)\right] < Y_t^+ \right. \\ &\quad \left. \leqslant E(Y_t^+) + \sqrt{V(Y_t^+)}\left[v_i^+ + \phi_H^{-1}\left(v_j^+ - v_i^+ + \frac{\Delta^+}{2}\right)\right]\right) \end{aligned} , \tag{13}$$

where $E(Y_t^+) = 1/\sqrt{2\pi}$ and $V(Y_t^+) = (\pi - 1)/2\pi$. For the proposed upper-sided ATEWMA $\bar{X}$ scheme, let us define,

$$A_1 = \frac{1}{\sqrt{2\pi}} + \sqrt{\frac{\pi - 1}{2\pi}} \left[v_i^+ + \phi_H^{-1} \left(v_j^+ - v_i^+ - \frac{\Delta^+}{2} \right) \right], \tag{14}$$

$$A_2 = \frac{1}{\sqrt{2\pi}} + \sqrt{\frac{\pi - 1}{2\pi}} \left[v_i^+ + \phi_H^{-1} \left(v_j^+ - v_i^+ + \frac{\Delta^+}{2} \right) \right]. \tag{15}$$

Therefore, the elements $q_{i,j}$ of matrix $\mathbf{Q}$ can be stated as,

$$q_{i,j} = \begin{cases} 0 & A_2 < 0 \\ \Phi(A_2 - \delta\sqrt{n}) & A_2 \geqslant 0 \text{ and } A_1 < 0 \\ \Phi(A_2 - \delta\sqrt{n}) - \Phi(A_1 - \delta\sqrt{n}) & A_2 \geqslant 0 \text{ and } A_1 \geqslant 0 \end{cases}, \tag{16}$$

where $\Phi(\cdot)$ represents the c.d.f. of the standard normal distribution, and δ is the magnitude of the standardized mean shift.

The ARL performance of control charts is commonly evaluated in the zero-state case. As defined by Dickinson et al. (2014), the *zero-state* ARL performance is based on the assumption that a shift in the parameter occurs at the beginning of the Phase II monitoring. Furthermore, the zero-state ARL value of the suggested upper-sided ATEWMA $\bar{X}$ scheme can be computed using,

$$\mathrm{ARL} = \mathbf{q}_z^{\mathsf{T}} (\mathbf{I} - \mathbf{Q})^{-1} \mathbf{1}, \tag{17}$$

where $\mathbf{q}_z = (q_{z_1}, q_{z_2}, \cdots, q_{z_m})^{\mathsf{T}}$ is the initial probabilities associated with m transient states for the zero-state case, and

$$q_{z_j} = \begin{cases} 1, & Q_0^+ \in E_j^+ \\ 0, & \text{otherwise} \end{cases}. \tag{18}$$

Compared with the zero-state case, the *steady-state* case is usually based on the assumption that the process remains at the in-control state at the start of Phase II monitoring, and then some random shift occurs later. This assumption makes the steady-state ARL performance of a scheme more realistic and informative than its corresponding zero-state counterpart. In the steady-state case, the ARL value of the proposed upper-sided ATEWMA $\bar{X}$ scheme can be defined as,

$$\mathrm{ARL} = \mathbf{q}_s^{\mathsf{T}}(\mathbf{I} - \mathbf{Q})^{-1}\mathbf{1}, \tag{19}$$

where $\mathbf{q}_s = (q_{s_1}, q_{s_2}, \cdots, q_{s_m})^{\mathsf{T}}$ is the steady-state initial probability vector of size m. A simplified procedure designed by Champ (1992) is considered here to directly calculate the steady-state initial probability vector $\mathbf{q}_s$, say,

$$\mathbf{q}_s = (\mathbf{1}^{\mathsf{T}}\mathbf{s})^{-1}\mathbf{s}. \tag{20}$$

As defined in Champ (1992),

$$\mathbf{s} = (\mathbf{G} - \mathbf{Q}^{\mathsf{T}})^{-1}\mathbf{U}, \tag{21}$$

where

$$\mathbf{G} = \begin{pmatrix} 2 & 1 & 1 & \cdots & 1 \\ 0 & 1 & 0 & \cdots & 0 \\ 0 & 0 & 1 & \cdots & 0 \\ \vdots & \vdots & \vdots & \ddots & \vdots \\ 0 & 0 & 0 & \cdots & 1 \end{pmatrix},$$

and $\mathbf{U} = (1, 0, 0, \cdots, 0)^{\mathsf{T}}$ is an $m \times 1$ column vector. Finally, one can easily compute both the zero-state and the steady-state ARL performance of the recommended upper-sided ATEWMA $\bar{X}$ scheme by using (17) and (19), respectively.

In general, the optimal design strategy of traditional control charts aims at finding a scheme that can provide the minimum out-of-control ARL (denoted as ARL_1) for a specified shift δ, with the constraint that an acceptable in-control ARL (denoted as ARL_0) is satisfied. This approach leads to a problem that the performance of a scheme with optimal parameters is extremely dependent on the specified magnitude of the shift δ. Moreover, in practice, the magnitude of a shift is rarely known in advance. Hence, it is necessary to design an optimal design strategy for the recommended one-sided ATEWMA $\bar{X}$ scheme to make it more sensitive in monitoring a wide range of shifts. Similar to the

optimal design strategy proposed in Capizzi & Masarotto (2003), the optimal design procedure of the recommended upper-sided ATEWMA $\bar{X}$ scheme for the zero-state case is summarized as follow s,

Step 1: Set a desired $\mathrm{ARL}_0 = C$, the sample size n, and two different designed shift values, i.e., a small mean shift δ_S, and a large mean shift δ_L.

Step 2: Based on the desired ARL_0, search the optimal parameters $\theta^* = \{H^+, \lambda, k\}$ of the proposed upper-sided ATEWMA $\bar{X}$ scheme providing the minimum ARL_1 for the specified large shift δ_L. In other words, the optimal parameters θ^* is the solution of the following nonlinear minimization problem, i.e.,

$$\begin{cases} \theta^* = \underset{\theta=\{H^+,\lambda,k\}}{\arg\min}\ \mathrm{ARL}_1(\theta, \delta_L, n). \\ \text{Subject to :} \\ \mathrm{ARL}(\theta^*, \delta_L = 0, n) = \mathrm{ARL}_0, \end{cases} \tag{22}$$

where the ARL value for the zero-state case can be computed using (17).

Step 3: Choose a small positive constant α (say, $\alpha = 0.05$ in this paper), and then find the solution Θ^* of the following nonlinear minimization problem, where Θ^* is defined here as the optimal parameters of the proposed upper-sided ATEWMA $\bar{X}$ scheme,

$$\begin{cases} \Theta^* = \underset{\Theta=\{H^+,\lambda,k\}}{\arg\min}\ \mathrm{ARL}_1(\Theta, \delta_S, n). \\ \text{Subject to :} \\ \mathrm{ARL}(\Theta^*, \delta_S = 0, n) = \mathrm{ARL}_0, \\ \text{and } \mathrm{ARL}_1(\Theta^*, \delta_L, n) \leqslant (1+\alpha) \times \mathrm{ARL}_1(\theta^*, \delta_L, n). \end{cases} \tag{23}$$

This means, find the optimal upper-sided ATEWMA $\bar{X}$ scheme with the minimum ARL_1 value at the small shift δ_S among those schemes for which the ARL_1 value at the large shift δ_L is "nearly minimum".

It must be noted that the optimal design procedure associated with the steady-state case is similar to the procedure introduced above, except that both ARL_0 and ARL_1 in Steps 2 and 3 should be computed using (19). Furthermore, for more details on how to solve the nonlinear minimization

problems (i.e., (22) and (23)) in the optimal design procedure presented above, readers can refer to the Appendix B.

4 Implementation of the VSI feature

Traditional control charts are commonly implemented by taking the observations from the process with a FSI feature. Conversely, VSI type schemes operate by varying the sampling interval as a function of the observations. By using the control limits (i.e., H^+ and H^-) and the corresponding warning limits (say, W^+ and W^-), the suggested one-sided ATEWMA $\bar{X}$ scheme with a VSI feature (i.e., the one-sided VSI-ATEWMA $\bar{X}$ scheme) can be partitioned into three regions, namely, the safe region, the warning region, and the out-of-control region. For simplicity, a flowchart for the VSI strategy of the proposed upper-sided VSI-ATEWMA $\bar{X}$ scheme is given as follow s,

(Please insert Figure 1 here)

Different from the ARL, the average time to signal (ATS) is a popular index for control charts with VSI feature, and it is defined as the average time from the beginning until the VSI type scheme generates a signal (see Li et al. (2014)). Note that the ATS of the recommended one-sided ATEWMA $\bar{X}$ scheme with the FSI feature is just a multiple of its ARL, i.e., $\mathrm{ATS}^{\mathrm{FSI}} = \mathrm{ARL}^{\mathrm{FSI}} \times d^{\mathrm{FSI}}$, where d^{FSI} denotes the fixed sampling interval used in the one-sided ATEWMA $\bar{X}$ scheme. But for the ATS of the suggested one-sided VSI-ATEWMA $\bar{X}$ scheme, it depends on both the ARL and the varying sampling intervals, say, $\mathrm{ATS}^{\mathrm{VSI}} = \mathrm{ARL}^{\mathrm{VSI}} \times E(d)$, where $E(d)$ is the average of sampling intervals d (i.e., d_L and d_S) used in the one-sided VSI-ATEWMA $\bar{X}$ scheme, and it is commonly considered to be $E(d) = 1$ time unit. The transition probability matrix $\mathbf{Q}$ developed in Section 3 can also be used to compute the ATS value of the recommended one-sided VSI-ATEWMA $\bar{X}$ scheme, except that the zero-state ATS value should be obtained through the following expression,

$$\mathrm{ATS} = \mathbf{q}_z^{\mathsf{T}}(\mathbf{I} - \mathbf{Q})^{-1}\mathbf{g}, \tag{24}$$

where $\mathbf{q}_z$ is an $m \times 1$ initial probability vector defined in (18) for the zero-state scenario. In addition, $\mathbf{g}$ is an $m \times 1$-dimensional sampling interval vector, and the elements g_j of $\mathbf{g}$ are,

$$g_j = \begin{cases} d_S, & v_j \in (W^+, H^+] \\ d_L, & v_j \in [-1/\sqrt{\pi - 1}, W^+] \end{cases}, \tag{25}$$

where v_j represents the midpoint value of the jth subinterval E_j^+.

Unlike the steady-state ARL, when computing the ATS value of the recommended one-sided VSI-ATEWMA $\bar{X}$ scheme in the steady-state case, it is necessary to consider the position where the shift occurs randomly, say, during a short or a long sampling interval. As a more realistic criterion in the steady-state case, the adjusted time to signal (AATS) is defined in Reynolds et al. (1988) as the length of time from the process shift to the scheme signals, and it can be obtained by using,

$$\mathrm{AATS} = \mathbf{q}_a^{\mathsf{T}} \left((\mathbf{I} - \mathbf{Q})^{-1} - \frac{1}{2}\mathbf{I} \right) \mathbf{g}, \tag{26}$$

where $\mathbf{q}_a$ represents an $m \times 1$-dimensional initial probability vector, and the jth element q_{a_j} of $\mathbf{q}_a$ can be defined as,

$$q_{a_j} = \frac{q_{s_j} \times g_j}{\mathbf{q}_s^{\mathsf{T}} \times \mathbf{g}}, \tag{27}$$

where q_{s_j} and g_j denote the jth element of $\mathbf{q}_s$ defined in (20) and the jth element of $\mathbf{g}$ defined in (25), respectively.

In order to provide a fair comparison between the one-sided VSI-ATEWMA $\bar{X}$ scheme and its FSI counterpart, $\mathrm{ATS}^{\mathrm{VSI}} = \mathrm{ATS}^{\mathrm{FSI}}$ is set. More specifically, $E(d) = p_S \times d_S + (1 - p_S) \times d_L = d^{\mathrm{FSI}} = 1$, where $d_L > 1$, and p_S denotes the probability of adopting the short sampling interval d_S. Furthermore, a two-stage optimal design procedure of the suggested upper-sided VSI-ATEWMA $\bar{X}$ scheme is given as follow s,

Step 1: Choose a desired $\mathrm{ARL}_0 = C$, the sample size n, a small mean shift value δ_S, and a large mean shift value δ_L. Additionlly, specify a short sampling interval d_S, and the probability p_S of adopting the short sampling interval.

Step 2: Based on the optimal design procedure developed in Section 3, search for the corresponding

$\Theta^* = \{H^+, \lambda, k\}$ of the proposed upper-sided VSI-ATEWMA $\bar{X}$ scheme with the constraint that the desired ARL_0 is satisfied.

Step 3: Compute the corresponding long sampling interval d_L by using,

$$d_L = \frac{E(d) - p_S \times d_S}{(1 - p_S)}, \tag{28}$$

where $E(d) = d^{\mathrm{FSI}} = 1$.

Step 4: Set the magnitude of the shift $\delta = 0$, and then determine the value of W^+ by solving the following problem,

$$\begin{cases} \mathrm{ATS}_0(W^+, \Theta^*, d_S, d_L, \delta = 0, n) = C. \\ \text{Subject to :} \\ \mathrm{ARL}_0(\Theta^*, \delta = 0, n) = C, \\ \text{and } E(d) = d^{\mathrm{FSI}} = 1. \end{cases} \tag{29}$$

Similar to the case of the proposed one-sided ATEWMA $\bar{X}$ chart with the FSI feature, the optimal design procedure introduced above for the zero-state case is also suitable for the steady-state case, except that the corresponding ARL and ATS_0 computations in Steps 2 and 4 should be replaced by (19) and (26), respectively. In what follows, the ARL and ATS are used to evaluate the detection capabilities of the upper-sided ATEWMA schemes with FSI and VSI features, respectively.

5 Comparative studies

Before conducting comparative studies, some comparisons of ARL (or the ATS) obtained using the Markov chain model and the Monte Carlo simulation, respectively, are provided in Table 1. Due to the space limitation, only four sets of optimal parameters associated with $(\delta_S, \delta_L) = (0.75, 2)$ are considered here for illustration. For example, $H^+ = 0.6346, \lambda = 0.0979, k = 8.8393, W^+ = -0.0315$ for the zero-state ATS with the sample size $n = 1$, and $H^+ = 0.5705, \lambda = 0.0617, k = 3.9254$ for the steady-state ARL with the sample size $n = 3$. Moreover, it is worth noting that the number of

subintervals m used in the Markov chain model is set as 201, and the the number of runs used in the Monte Carlo simulation is 10^5. As we can see from Table 1, the largest discrepancy between these two methods is approximately 0.5% of the ARL (or ATS). This fact means that the Markov chain model established in this paper obtains a good agreement with the Monte Carlo simulation, and $m = 201$ seems to be sufficient for most computations.

(Please insert Table 1here)

Two competing control charts, namely, (1) the conventional AEWMA $\bar{X}$ scheme, and (2) the one-sided TEWMA $\bar{X}$ scheme, are used in this paper for comparison with the recommended one-sided ATEWMA $\bar{X}$ scheme. Meanwhile, the corresponding VSI counterparts of these two competing schemes are also respectively used to compare with the suggested one-sided VSI-ATEWMA $\bar{X}$ scheme in terms of the ATS and the AATS. Due to the space limitation, only the performance comparisons of the upper-sided ATEWMA $\bar{X}$ and VSI-ATEWMA $\bar{X}$ schemes with $n = 1$ and $n = 3$ are shown in this Section. For more details about the Markov chain models used in the conventional AEWMA $\bar{X}$ scheme, the one-sided TEWMA $\bar{X}$ scheme, and the VSI-AEWMA $\bar{X}$ scheme, readers can refer to Capizzi & Masarotto (2003), Shu et al. (2007) and Tang et al. (2017), respectively. Furthermore, to provide a fair comparison, all these mentioned schemes are designed based on a desired $\mathrm{ARL}_0 = \mathrm{ATS}_0 = 370$, and $m = 201$. It is also worth noting that, as the comparison schemes, both the conventional AEWMA $\bar{X}$ scheme and the VSI-AEWMA $\bar{X}$ scheme also utilize the optimal design procedures developed for the one-sided ATEWMA $\bar{X}$ scheme and the one-sided VSI-ATEWMA $\bar{X}$ scheme, respectively, to search for their optimal parameters.

The zero-state and the steady-state optimal parameters of the proposed upper-sided ATEWMA $\bar{X}$ scheme, the conventional AEWMA $\bar{X}$ scheme, and the upper-sided TEWMA $\bar{X}$ scheme are, respectively, listed in Tables 2 and 3, for different pre-specified upward mean shifts. For example, when the specified shift combination $(\delta_S, \delta_L) = (0.25, 2)$, the zero-state optimal parameters $\{H^+, \lambda, k\}$ of the proposed upper-sided ATEWMA $\bar{X}$ scheme for $n = 3$ are $\{0.4553, 0.0420, 3.9207\}$. Meanwhile, the corresponding zero-state optimal parameters $\{H', \lambda', k'\}$ of the conventional AEWMA $\bar{X}$ scheme for $n = 3$ are $\{0.4508, 0.0457, 2.8025\}$, where λ' is the smoothing factor of the conventional AEWMA $\bar{X}$ scheme, and the corresponding upper and lower control limits are $\mathrm{UCL} = H'$

and $\mathrm{LCL} = -H'$, respectively. Additionally, for the existing upper-sided TEWMA $\bar{X}$ scheme, the zero-state optimal parameters $\{r, h^+\}$ for $n = 3$ are $\{0.7578, 3.1319\}$ when the designed mean shift $\delta_T = 2$, where δ_T is a particular shift size for which the upper-sided TEWMA $\bar{X}$ scheme is optimally designed, and r and h^+ represent the smoothing factor and the upper control limit of the upper-sided TEWMA $\bar{X}$ scheme, respectively (see Table 2).

(Please insert Table 2 and Table 3 here)

To evaluate the ARL performance of the recommended upper-sided ATEWMA $\bar{X}$ scheme and the conventional AEWMA $\bar{X}$ scheme, both the zero-state and the steady-state ARL values of these two schemes for detecting different mean shifts $\delta \in \{0.25, 0.5, 0.75, 1, 1.25, 1.5, 1.75, 2, 2.5, 3\}$ are listed in Tables 4 and 5, respectively, with the constraint on the desired $\mathrm{ARL}_0 = 370$. For instance, if both of these two schemes are designed based on $(\delta_S, \delta_L) = (0.5, 2)$ and $n = 1$, the ARL_1 values of the upper-sided ATEWMA $\bar{X}$ scheme and the AEWMA $\bar{X}$ scheme in the zero-state case for $\delta = 1$ are 8.35 and 9.59, respectively (see Table 4), and the corresponding steady-state ARL_1 values of these two schemes for $\delta = 1$ are 8.43 and 9.55, respectively (see Table 5).

(Please insert Table 4 and Table 5 here)

As it can be drawn from Tables 4 and 5,

- Irrespective of the zero-state or the steady-state cases, the proposed upper-sided ATEWMA $\bar{X}$ scheme works better than the conventional AEWMA $\bar{X}$ scheme in monitoring the whole upward shift domain, especially in the small mean shift range.

- For each mean shift combination (δ_S, δ_L), both the zero-state and the steady-state ARL values of the proposed upper-sided ATEWMA $\bar{X}$ scheme and the conventional AEWMA $\bar{X}$ scheme tend to be similar, as the magnitude of the upward mean shift δ increases. For example, when $(\delta_S, \delta_L) = (0.5, 3)$ and $n = 3$, the zero-state ARL values of the upper-sided ATEWMA $\bar{X}$ scheme and the AEWMA $\bar{X}$ scheme for $\delta = 0.25$ are 35.98 and 40.52, respectively. Then, as δ increases to 3, the corresponding zero-state ARL values of these two charts become 1.02 and 1.05, respectively.

On the other hand, to provide some intuitive comparisons between the recommended upper-sided ATEWMA $\bar{X}$ scheme and the upper-sided TEWMA $\bar{X}$ scheme, both the zero-state and the steady-state ARL curves of these two schemes for $n \in \{1, 3\}$ are presented in Figures 2 and 3, respectively. It is worth noting that the ARL scale in these figures is chosen to be logarithmic. Due to the space limitation, only the upper-sided ATEWMA $\bar{X}$ scheme designed based on $(\delta_S, \delta_L) = (0.5, 2)$ is considered here for illustration. Additionally, three competing upper-sided TEWMA $\bar{X}$ schemes in Figures 2 and 3 are, respectively, designed to generate the minimum ARL_1 values for different specified upward mean shifts $\delta_T \in \{0.5, 1.25, 2.0\}$.

(Please insert Figure 2 and Figure 3 here)

As it is shown in Figures 2 and 3, the suggested upper-sided ATEWMA $\bar{X}$ scheme can provide a balanced protection against both small and large upward shifts simultaneously. In other words, the upper-sided ATEWMA $\bar{X}$ scheme performs better than the upper-sided TEWMA $\bar{X}$ scheme in detecting a mean shift δ that is much larger or smaller than the designed size δ_T, especially for the case of sample size $n > 1$. For instance, the proposed upper-sided ATEWMA $\bar{X}$ scheme and the upper-sided TEWMA $\bar{X}$ scheme designed for $\delta_T = 0.5$ have almost the same steady-state ARL profiles when the sample size $n = 3$ and the magnitude s of the upward shift $\delta < 1$. But if a large upward shift (say, $\delta > 2$) occurs, the proposed scheme can provide a more effective protection than the upper-sided TEWMA $\bar{X}$ scheme designed for $\delta_T = 0.5$ (see Figure 3 (d)).

For the upper-sided VSI-ATEWMA $\bar{X}$ scheme and the other two competing schemes with the VSI feature, two sampling intervals, say, $d_S = 0.3$ and $d_L = 1.7$, are used here for illustration. Following the two-stage optimal design procedure introduced in Section 4, both the zero-state and the steady-state optimal parameters of the recommended upper-sided VSI-ATEWMA $\bar{X}$ scheme, the conventional VSI-AEWMA $\bar{X}$ scheme, and the upper-sided VSI- TEWMA $\bar{X}$ scheme are listed in Tables 6 and 7, respectively. For example, for the specified shift combination $(\delta_S, \delta_L) = (0.25, 3)$ and the shift size $n = 3$, the steady-state optimal parameters $\{H^+, \lambda, k, W^+\}$ of the proposed upper-sided VSI-ATEWMA $\bar{X}$ scheme are $\{0.6516, 0.1006, 5.5516, -0.0459\}$, and the corresponding steady-state optimal parameters $\{H', \lambda', k', w'\}$ of the conventional VSI-AEWMA $\bar{X}$ scheme are $\{0.5407, 0.0780, 3.3726, 0.2314\}$. Note that the upper (or lower) warning control limit of the conven-

tional VSI-AEWMA $\bar{X}$ scheme are defined as $\mathrm{UWL} = w' \times H'$ and $\mathrm{LWL} = -w' \times H'$, respectively, where w' is a constant implemented to determine the proportion of time used for the short or the long sampling interval. Additionally, when the sample size $n = 3$ and the specific shift $\delta_T = 1.5$, the steady-state optimal parameters $\{r, h^+, w^+\}$ of the upper-sided VSI- TEWMA $\bar{X}$ scheme are $\{0.5291, 2.2975, -0.1770\}$ (see Table 7). It must be noted that, due to the implementation of the truncation method, the warning control limits of the proposed upper-sided VSI-ATEWMA $\bar{X}$ scheme are all negative. This fact implies that the initial sampling interval used in the proposed scheme for the zero-state case is $d_0 = d_S$. Conversely, if we do not expressly set $d_0 = d_S$, the initial sampling interval used in the conventional VSI-AEWMA $\bar{X}$ scheme for the zero-state case is $d_0 = d_L$. In this context, for a more comprehensive comparison, the zero-state optimal parameters of the conventional VSI-AEWMA $\bar{X}$ scheme for both $d_0 = d_L$ and $d_0 = d_S$ are provided in Table 6.

(Please insert Table 6 and Table 7 here)

For comparison, both the zero-state and the steady-state ATS profiles of the proposed upper-sided VSI-ATEWMA $\bar{X}$ scheme, the conventional VSI-AEWMA $\bar{X}$ scheme, and the upper-sided FSI-ATEWMA $\bar{X}$ scheme for $n \in \{1, 3\}$ are presented in Tables 8 and 9, respectively. As it is expected, irrespective of the zero-state or the steady-state case, the proposed upper-sided VSI-ATEWMA $\bar{X}$ scheme performs better than its FSI counterpart in terms of the ATS and the AATS. Furthermore, the suggested upper-sided VSI-ATEWMA $\bar{X}$ scheme in the zero-state case is uniformly more sensitive than the conventional VSI-AEWMA $\bar{X}$ scheme using $d_0 = d_L$ or $d_0 = d_S$ (see Table 8). Meanwhile, the proposed upper-sided VSI-ATEWMA $\bar{X}$ scheme in the steady-state case is superior to the conventional VSI-AEWMA $\bar{X}$ scheme in most scenarios, except that in several large upward mean shift detections. For example, when $(d_S, d_L) = (0.75, 3)$ and $n = 3$, the AATS values of the upper-sided VSI-ATEWMA $\bar{X}$ scheme and the VSI-AEWMA $\bar{X}$ scheme for $\delta = 3$ are 0.76 and 0.75, respectively (see Table 9).

(Please insert Table 8 and Table 9 here)

The ATS and AATS comparisons between the upper-sided VSI-ATEWMA $\bar{X}$ scheme and the upper-sided VSI- TEWMA $\bar{X}$ scheme are shown in Figures 4 and 5, respectively. Similar to the settings in the FSI case s, the upper-sided VSI-ATEWMA $\bar{X}$ scheme is designed based on $(\delta_S, \delta_L) =$

$(0.5, 2)$, and both the zero-state and the steady-state optimal parameters of this proposed scheme can be obtained from Tables 6 and 7, respectively. Meanwhile, three different upper-sided VSI- TEWMA $\bar{X}$ schemes designed assuming $\delta_T \in \{0.5, 1.25, 2.0\}$ are plotted in Figures 4 and 5, respectively, for comparison. It can be observed that, irrespective of the zero-state or the steady-state case, the competing upper-sided VSI- TEWMA $\bar{X}$ schemes can provide slightly better performance than the suggested upper-sided VSI-ATEWMA $\bar{X}$ scheme, as long as an upward mean shift δ is near the designed shift size δ_T, but the proposed upper-sided VSI-ATEWMA $\bar{X}$ scheme works better than the upper-sided VSI- TEWMA $\bar{X}$ scheme in detecting an upward mean shift δ that is much larger or smaller than the designed size δ_T.

(Please insert Figure 4 and Figure 5 here)

6 A numerical example

This example aims to illustrate the implementation of the recommended upper-sided ATEWMA $\bar{X}$ scheme for upward shift detection. The simulated dataset s employed in this paper are similar to the one in Tang et al. (2017), which consists of 25 samples generated from a normal distribution $N(100, 3)$. Two different scenarios are assumed in this illustrative example, say,

- the zero-state scenario: all 25 samples of the datasets are adjusted with either $0.75 \times \sigma_0$ or $2 \times \sigma_0$ upward mean shift;
- the steady-state scenario: only the last 15 samples of the datasets are adjusted with either $0.75 \times \sigma_0$ or $2 \times \sigma_0$ upward mean shift,

For comparison, the conventional AEWMA $\bar{X}$ scheme and the upper-sided TEWMA $\bar{X}$ scheme are constructed in this example. The desired ARL_0 values of these three schemes are all set at 370. For the shift combination $(\delta_S, \delta_L) = (0.75, 2)$ and the sample size $n = 1$, it is easy to obtain from Tables 2 and 3 that, the zero-state and steady-state optimal parameters $\{H^+, \lambda, k\}$ of the proposed upper-sided ATEWMA $\bar{X}$ scheme are $\{0.6346, 0.0979, 8.8393\}$ and $\{0.6802, 0.1071, 8.6228\}$, respectively. Meanwhile, the zero-state and steady-state optimal parameters $\{H', \lambda', k'\}$ of the conventional AEWMA $\bar{X}$ scheme are $\{0.7481, 0.1353, 8.1341\}$ and $\{0.6525, 0.1081, 4.4318\}$, respectively,

and the corresponding optimal parameters $\{r, h^+\}$ of the upper-sided TEWMA $\bar{X}$ scheme designed for $\delta_T = 1.5$ are $\{0.2043, 1.1003\}$ and $\{0.2251, 1.1841\}$, respectively. Irrespective of the zero-state or the steady-state cases, the datasets and the corresponding charting statistics are presented in Table 10.

(Please insert Table 10 here)

The upper-sided ATEWMA $\bar{X}$ scheme, the AEWMA $\bar{X}$ scheme, and the upper-sided TEWMA $\bar{X}$ scheme for monitoring the zero-state (or the steady-state) datasets with $\delta = 0.75 \times \sigma_0$ and $\delta = 2 \times \sigma_0$ are presented in Figure 6 (Figure 7), respectively. The control chart triggers an out-of-control signal if a charting statistic plots outside the control limit.

- As it can be seen in Figure 6, when the zero-state dataset with upward shift $\delta = 0.75 \times \sigma_0$ is monitored, the proposed upper-sided ATEWMA $\bar{X}$ scheme gives an out-of-control signal at the 13th observation, while the conventional AEWMA $\bar{X}$ scheme and the upper-sided TEWMA $\bar{X}$ scheme all signal at the 16th observation (see Figure 6 (a), (b), and (c)). Meanwhile, if the upward shift in zero-state dataset corresponds to $\delta = 2 \times \sigma_0$, the proposed upper-sided ATEWMA $\bar{X}$ scheme generates an out-of-control signal at the 7th observation, while the conventional AEWMA scheme $\bar{X}$ and the upper-sided TEWMA $\bar{X}$ scheme all signal at the 9th observation (see Figure 6 (d), (e), and (f)). This indicates that the recommended upper-sided ATEWMA $\bar{X}$ scheme in the zero-state case of this example outperforms the conventional AEWMA $\bar{X}$ scheme and the upper-sided TEWMA $\bar{X}$ scheme in monitoring the small and the large upward mean shifts simultaneously.

- For the steady-state case shown in Figure 7, the proposed upper-sided ATEWMA $\bar{X}$ scheme gives an out-of-control signal at the 22th observation when the upward shift $\delta = 0.75 \times \sigma_0$, and the conventional AEWMA $\bar{X}$ scheme and the upper-sided TEWMA $\bar{X}$ scheme all signal at the 25th observation (see Figure 7 (a), (b), and (c)). Additionally, for the upward shift $2 \times \sigma_0$ scenario, the proposed upper-sided ATEWMA $\bar{X}$ scheme generates an out-of-control signal at the 13th observation, while the conventional AEWMA $\bar{X}$ scheme signals at the 15th observation, and the upper-sided TEWMA $\bar{X}$ scheme signals at the 14th observation (see Figure 7 (d), (e), and (f)). This means that, in the steady-state case of this example, the upper-

sided ATEWMA $\bar{X}$ scheme is also superior to the AEWMA $\bar{X}$ scheme and the upper-sided TEWMA $\bar{X}$ scheme in monitoring the small and the large upward mean shifts simultaneously.

(Please insert Figure 6 and Figure 7 here)

Note that all the charting statistics that are detected to be out-of-control are in bold in Table 10. In addition, it can be observed from Figure 7 (a) and (b) that the conventional AEWMA $\bar{X}$ scheme with a small smoothing parameter λ' takes a longer time than the proposed upper-sided ATEWMA $\bar{X}$ scheme to detect the upward mean shift, when a Q_t value of the conventional AEWMA statistic is closer to LCL. This means that the proposed upper-sided ATEWMA $\bar{X}$ scheme seems to be able to avoid the inertia problem better than the conventional AEWMA $\bar{X}$ scheme, and this could be an interesting problem for future research.

7 Conclusion

In this study, we proposed a new one-sided ATEWMA $\bar{X}$ scheme that combines a Shewhart $\bar{X}$ scheme and a one-sided TEWMA $\bar{X}$ scheme in a smooth way for a rapid upward (or downward) shift detection. Similar to the one-sided TEWMA scheme developed by Shu et al. (2007), a truncation method is employed in the proposed one-sided ATEWMA $\bar{X}$ scheme to improve its detection efficiency. The basic idea of the truncation method for the suggested upper-sided (lower-sided) ATEWMA $\bar{X}$ scheme is to truncate the sample means $\bar{X}$ below (or above) the in-control mean μ_0 to the value of μ_0, and then to accumulate the sample means $\bar{X}$ above (below) the in-control mean μ_0 only. A dedicated Markov chain model has been established to evaluate the RL properties of the recommended one-sided ATEWMA $\bar{X}$ scheme, and the corresponding optimal design procedure of this recommended scheme has also been presented based on the ARL criteria. Furthermore, a VSI feature has been integrated into the recommended one-sided ATEWMA $\bar{X}$ scheme for improving the sensitivity of the scheme in detecting either upward or downward mean shifts. Numerical results showed that the recommended one-sided ATEWMA $\bar{X}$ scheme with optimal parameters is uniformly more sensitive than the conventional AEWMA $\bar{X}$ scheme in monitoring upward mean shifts, especially for small mean shift range. In addition, compared with the one-sided TEWMA $\bar{X}$ scheme, the proposed one-sided

ATEWMA $\bar{X}$ scheme can provide good protection against both small and large mean shifts simultaneously. In other words, it works better than the one-sided TEWMA $\bar{X}$ scheme in monitoring an upward mean shift δ that is much larger or smaller than δ_T. It is also indicated that the VSI feature can substantially improve the detection efficiency of the recommended one-sided ATEWMA $\bar{X}$ scheme. Comparisons with other competing VSI type charts also showed that the suggested one-sided VSI-ATEWMA $\bar{X}$ scheme can provide a better overall performance for a wide range of mean shifts.

A possible future extension for the current research is to investigate the RL properties of the recommended one-sided ATEWMA $\bar{X}$ scheme in the worst-case scenario. Meanwhile, similar to Li et al. (2009), the necessary and sufficient conditions for non-interaction of the suggested upper-sided and lower-sided ATEWMA $\bar{X}$ schemes are also worth studying. Finally, the suggested one-sided ATEWMA $\bar{X}$ scheme with estimated parameters could also be considered.

Disclosure statement

No potential conflict of interest was reported by the author(s).

Funding

This work was supported by National Natural Science Foundation of China (Grant number: 71802110, 71872088); Humanity and Social Science Foundation of Ministry of Education of China (Grant number:19YJA630061); China Scholarship Council (Grant number: 202006840086); Postgraduate Research & Practice Innovation Program of Jiangsu Province (Grant number: KYCX21_0306); Key Research Base of Philosophy and Social Sciences in Jiangsu Information Industry Integration Innovation and Emergency Management Research Center.

References

Anwar, S. M., Aslam, M., Ahmad, S., & Riaz, M. (2020). A modified-mxEWMA location chart for the improved process monitoring using auxiliary information and its application in wood industry. *Quality Technology & Quantitative Management*, *17*, 561–579.

Barr, D. R., & Sherrill, E. T. (1999). Mean and variance of truncated normal distributions. *The American Statistician*, *53*, 357–361.

Capizzi, G., & Masarotto, G. (2003). An adaptive exponentially weighted moving average control chart. *Technometrics*, *45*, 199–207.

Castagliola, P., Tran, K., Celano, G., Rakitzis, A., & Maravelakis, P. (2019). An EWMA-type sign chart with exact run length properties. *Journal of Quality Technology*, *51*, 51–63.

Champ, C. W. (1992). Steady-state run length analysis of a Shewhart quality control chart with supplementary runs rules. *Communications in Statistics–Theory and Methods*, *21*, 765–777.

Champ, C. W., Woodall, W. H., & Mohsen, H. A. (1991). A generalized quality control procedure. *Statistics & Probability Letters*, *11*, 211–218.

Chong, N. L., Khoo, M. B., Castagliola, P., Saha, S., & Mim, F. N. (2020). A variable parameters auxiliary information based quality control chart with application in a spring manufacturing process: The Markov chain approach. *Quality Engineering*, (pp. 1–19).

Dickinson, R. M., Roberts, D. A. O., Driscoll, A. R., Woodall, W. H., & Vining, G. G. (2014). CUSUM charts for monitoring the characteristic life of censored Weibull lifetimes. *Journal of Quality Technology*, *46*, 340–358.

Gan, F. (1998). Designs of one-and two-sided exponential EWMA charts. *Journal of Quality Technology*, *30*, 55–69.

Haq, A. (2019). Weighted adaptive multivariate CUSUM charts with variable sampling intervals. *Journal of Statistical Computation and Simulation*, *89*, 478–491.

Haq, A. (2020). One-sided and two one-sided MEWMA charts for monitoring process mean. *Journal of Statistical Computation and Simulation*, *90*, 699–718.

Haq, A., Akhtar, S., & Boon Chong Khoo, M. (2021). Adaptive CUSUM and EWMA charts with auxiliary information and variable sampling intervals for monitoring the process mean. *Quality and Reliability Engineering International*, *37*, 47–59.

Haq, A., & Khoo, M. B. (2020). A parameter-free adaptive EWMA mean chart. *Quality Technology & Quantitative Management*, *17*, 528–543.

Hu, X., Castagliola, P., Zhou, X., & Tang, A. (2019). Conditional design of the EWMA median chart with estimated parameters. *Communications in Statistics–Theory and Methods*, *48*, 1871–1889.

Li, Z., Wang, Z., & Wu, Z. (2009). Necessary and sufficient conditions for non-interaction of a pair of one-sided EWMA schemes with reflecting boundaries. *Statistics & Probability Letters*, *79*, 368–374.

Li, Z., Zou, C., Gong, Z., & Wang, Z. (2014). The computation of average run length and average time to signal: an overview. *Journal of Statistical Computation and Simulation*, *84*, 1779–1802.

Liang, J. J., Qin, A. K., Suganthan, P. N., & Baskar, S. (2006). Comprehensive learning particle swarm optimizer for global optimization of multimodal functions. *IEEE Transactions on Evolutionary Computation*, *10*, 281–295.

Liu, L., Chen, B., Zhang, J., & Zi, X. (2015). Adaptive phase II nonparametric EWMA control chart with variable sampling interval. *Quality and Reliability Engineering International*, *31*, 15–26.

Montgomery, D. C. (2012). *Introduction to statistical quality control*. (Seventh ed.). New York: John Wiley & Sons.

Perry, M. B. (2020). An EWMA control chart for categorical processes with applications to social network monitoring. *Journal of Quality Technology*, *52*, 182–197.

Psarakis, S. (2015). Adaptive control charts: recent developments and extensions. *Quality and Reliability Engineering International*, *31*, 1265–1280.

Reynolds, M. R., Amin, R. W., Arnold, J. C., & Nachlas, J. A. (1988). $\bar{X}$ charts with variable sampling intervals. *Technometrics*, *30*, 181–192.

Reynolds Jr, M. R. (1989). Optimal variable sampling interval control charts. *Sequential Analysis*, *8*, 361–379.

Reynolds Jr, M. R., & Arnold, J. C. (2001). EWMA control charts with variable sample sizes and variable sampling intervals. *IIE Transactions*, *33*, 511–530.

Saccucci, M. S., Amin, R. W., & Lucas, J. M. (1992). Exponentially weighted moving average control schemes with variable sampling intervals. *Communications in Statistics–Simulation and Computation*, *21*, 627–657.

Shi, Y., & Eberhart, R. (1998). A Modified Particle Swarm Optimizer. In *1998 IEEE international conference on evolutionary computation proceedings. IEEE world congress on computational intelligence (Cat. No. 98TH8360)* (pp. 69–73). IEEE.

Shu, L. (2008). An adaptive exponentially weighted moving average control chart for monitoring process variances. *Journal of Statistical Computation and Simulation*, *78*, 367–384.

Shu, L., & Jiang, W. (2008). A new EWMA chart for monitoring process dispersion. *Journal of Quality Technology*, *40*, 319–331.

Shu, L., Jiang, W., & Wu, S. (2007). A one-sided EWMA control chart for monitoring process means. *Communications in Statistics–Simulation and Computation*, *36*, 901–920.

Shu, L., Jiang, W., & Wu, Z. (2012). Exponentially weighted moving average control charts for monitoring increases in Poisson rate. *IIE Transactions*, *44*, 711–723.

Su, Y., Shu, L., & Tsui, K. L. (2011). Adaptive EWMA procedures for monitoring processes subject to linear drifts. *Computational Statistics & Data Analysis*, *55*, 2819–2829.

Tang, A., Castagliola, P., Hu, X., & Sun, J. (2019a). The adaptive EWMA median chart for known and estimated parameters. *Journal of Statistical Computation and Simulation*, *89*, 844–863.

Tang, A., Castagliola, P., Hu, X., & Sun, J. (2019b). The performance of the adaptive EWMA median chart in the presence of measurement error. *Quality and Reliability Engineering International*, *35*, 423–438.

Tang, A., Castagliola, P., Sun, J., & Hu, X. (2017). An adaptive exponentially weighted moving average chart for the mean with variable sampling intervals. *Quality and Reliability Engineering International*, *33*, 2023–2034.

Tang, A., Castagliola, P., Sun, J., & Hu, X. (2019c). Optimal design of the adaptive EWMA chart for the mean based on median run length and expected median run length. *Quality Technology & Quantitative Management*, *16*, 439–458.

Tang, A., Sun, J., Hu, X., & Castagliola, P. (2019d). A new nonparametric adaptive EWMA control chart with exact run length properties. *Computers & Industrial Engineering*, *130*, 404–419.

Wang, H., Sun, H., Li, C., Rahnamayan, S., & Pan, J. (2013). Diversity enhanced particle swarm optimization with neighborhood search. *Information Sciences*, *223*, 119–135.

Zhang, L., & Chen, G. (2004). EWMA charts for monitoring the mean of censored Weibull lifetimes. *Journal of Quality Technology*, *36*, 321–328.

Zhou, W., Wang, Z., & Xie, W. (2020). Weighted signal-to-noise ratio robust design for a new double sampling np_x chart. *Computers & Industrial Engineering*, *139*, 106–124.

Appendix A

Similar to the recommended upper-sided ATEWMA $\bar{X}$ scheme, the in-control region of the proposed lower-sided ATEWMA $\bar{X}$ scheme is $\left[H^-, \frac{1}{\sqrt{\pi-1}}\right]$, and the width of each subinterval is given as $\Delta^- = (\frac{1}{\sqrt{\pi-1}} - H^-)/m$. The charting statistic Q_t^- of the proposed lower-sided ATEWMA $\bar{X}$ scheme is said to be in transient state j, at sampling point t, when $v_j^- - \frac{\Delta^-}{2} < Q_t^- \leqslant v_j^- + \frac{\Delta^-}{2}$, where $j = 1, 2, \cdots, m$, and $v_j^- = \frac{1}{\sqrt{\pi-1}} - (j - \frac{1}{2})\Delta^-$ represents the midpoint value of the jth subinterval $E_j^- = \left[v_j^- - \frac{\Delta^-}{2}, v_j^- + \frac{\Delta^-}{2}\right]$. Therefore, the corresponding elements $q_{i,j}$ of the matrix $\mathbf{Q}$ can be computed as follow s,

$$
\begin{aligned}
q_{i,j} &= \Pr\left(Q_t^- \in \text{state } j \;\middle|\; Q_{t-1}^- \in \text{state } i\right) \\
&= \Pr\left(v_j^- - v_i^- - \frac{\Delta^-}{2} < \phi_H(Z_t^- - v_i^-) \leqslant v_j^- - v_i^- + \frac{\Delta^-}{2}\right) \\
&= \Pr\left(v_i^- + \phi_H^{-1}\left(v_j^- - v_i^- - \frac{\Delta^-}{2}\right) < Z_t^- \leqslant v_i^- + \phi_H^{-1}\left(v_j^- - v_i^- + \frac{\Delta^-}{2}\right)\right), \qquad \text{(A.1)} \\
&= \Pr\left(E(Y_t^-) + \sqrt{V(Y_t^-)}\left[v_i^- + \phi_H^{-1}\left(v_j^- - v_i^- - \frac{\Delta^-}{2}\right)\right] < Y_t^- \right. \\
&\quad \left. \leqslant E(Y_t^-) + \sqrt{V(Y_t^-)}\left[v_i^- + \phi_H^{-1}\left(v_j^- - v_i^- + \frac{\Delta^-}{2}\right)\right]\right)
\end{aligned}
$$

where $\phi_H^{-1}(\cdot)$ is the Huber's inverse function defined in (12), $E(Y_t^-) = -1/\sqrt{2\pi}$ and $V(Y_t^-) = (\pi - 1)/2\pi$ denote the in-control mean and variance of the random variable Y_t^-, respectively. Then, let,

$$
A_3 = \frac{-1}{\sqrt{2\pi}} + \sqrt{\frac{\pi-1}{2\pi}}\left[v_i^- + \phi_H^{-1}\left(v_j^- - v_i^- - \frac{\Delta^-}{2}\right)\right], \qquad \text{(A.2)}
$$

$$
A_4 = \frac{-1}{\sqrt{2\pi}} + \sqrt{\frac{\pi-1}{2\pi}}\left[v_i^- + \phi_H^{-1}\left(v_j^- - v_i^- + \frac{\Delta^-}{2}\right)\right]. \qquad \text{(A.3)}
$$

Furthermore, the elements $q_{i,j}$ of the matrix $\mathbf{Q}$ are,

$$q_{i,j} = \begin{cases} 0, & A_3 > 0 \\ 1 - \Phi(A_3 + \delta\sqrt{n}), & A_3 \leqslant 0 \text{ and } A_4 > 0 \\ \Phi(A_4 + \delta\sqrt{n}) - \Phi(A_3 + \delta\sqrt{n}), & A_3 \leqslant 0 \text{ and } A_4 \leqslant 0 \end{cases}, \tag{A.4}$$

By using (17), (19), (24) and (26), the ARL and ATS values of the proposed lower-sided ATEWMA $\bar{X}$ scheme in both the zero-state and the steady-state cases can also be easily computed, except that the corresponding elements of $\mathbf{q}_z$ and $\mathbf{g}$ in (19) and (26) should be replaced by using,

$$q_{z_j} = \begin{cases} 1, & Q_0^- \in E_j^- \\ 0, & \text{otherwise} \end{cases}, \tag{A.5}$$

and

$$g_j = \begin{cases} d_S, & v_j \in [H^-, W^-) \\ d_L, & v_j \in [W^-, 1/\sqrt{\pi - 1}] \end{cases}, \tag{A.6}$$

respectively, where $Q_0^- = 0$.

Appendix B

In order to solve (22) and (23), a hybrid particle swarm optimization algorithm, named DNSPSO algorithm, is used here to obtain the optimal parameters of the one-sided ATEWMA $\bar{X}$ scheme. The DNSPSO algorithm has been firstly introduced by Wang et al. (2013), who suggested using one diversity enhancing mechanism and two neighborhood search strategies, to achieve a trade-off between exploration and exploitation abilities. The basic idea of the DNSPSO algorithm is to select a better particle between P_i and TP_i as the new particle P_i after updating the fitness values, and then two neighborhood search strategies are conducted with a certain probability to avoid a premature convergence. The pseudocode of the DNSPSO algorithm used in this paper is given as follows:

(Please insert the pseudocode here)

where N is the number of particles in the swarm, $i = 1, 2, \cdots, N$, and $j = 1, 2, \cdots, D$, where D is the dimension of the nonlinear minimization problem. Meanwhile, $OV_i = (ov_{i,1}, ov_{i,2}, \cdots, ov_{i,D})$

and $OX_i = (ox_{i,1}, ox_{i,2}, \cdots, ox_{i,D})$ denote the velocity and position of the ith particle P_i, respectively, $pbest_i = (pbest_{i,1}, pbest_{i,2}, \cdots, pbest_{i,D})$ represents the best previous position associated with the best fitness value for the ith particle, and $gbest = (gbest_1, gbest_2, \cdots, gbest_D)$ is the global best particle found by all particles so far. In addition, w_a is the inertia factor used to balance the global and local search abilities of particles, c_1 and c_2 are two positive constants, representing the weight of the "cognitive" and "social" components, respectively (see Shi & Eberhart (1998)). $rand1_{i,j}$ and $rand2_{i,j}$ are two random numbers within $[0, 1]$, and t is the iteration number. Moreover, FEs and MaxFEs denote the number and maximum number of function evaluations, respectively. $rand_j(0, 1)$ is a uniform random number within $[0, 1]$, and p_r is a predefined probability used to control the swarm diversity, $f_a(\cdot)$ is the fitness evaluation function, and p_{ns} is the probability of conducting a neighborhood search. Furthermore, OX_c and OX_d are the position vectors of two random particles in the k_n-neighborhood radius of P_i, where $k_n \in [0, \frac{N-1}{2}]$, $c, d \in [i - k_n, i + k_n] \wedge c \neq d \neq i$. r_1, r_2, and r_3 are three uniform random numbers within $(0, 1)$, such that $r_1 + r_2 + r_3 = 1$. Note that r_1, r_2, and r_3 are the same for all $j = 1, 2, \cdots, D$. Similarly, OX_e, OX_f are the position vectors of two random particles chosen for the entire swarm, $e, f \in [1, N] \wedge e \neq f \neq i$, r_4, r_5, and r_6 are three uniform random numbers within $(0, 1)$, such that $r_4 + r_5 + r_6 = 1$. Also, r_4, r_5, and r_6 are the same for all $j = 1, 2, \cdots, D$, and they are generated anew in each generation. For more details about the DNSPSO algorithm, readers can refer to Wang et al. (2013).

According to Liang et al. (2006) and Tang et al. (2019b), a population size $N = 20$ is sufficient for the case of $D = 3$ (i.e., in our case, three design parameters H^+ (or H^-), λ, and k of the proposed one-sided ATEWMA $\bar{X}$ scheme). Additionally, the other parameters, $w_a = 0.7298$ $c_1 = c_2 = 1.49618$, $k_n = 2$, $p_r = 0.3$, $p_{ns} = 0.8$, and $\mathrm{MaxFEs} = 5000$, are considered here to find the optimal parameters Θ^* of the proposed one-sided ATEWMA $\bar{X}$ scheme with the DNSPSO algorithm. Furthermore, for the proposed one-sided VSI-ATEWMA $\bar{X}$ scheme, once the optimal parameters Θ^* searched by the DNSPSO algorithm is given, it is easy to find the warning control limit W^+ of the scheme by using either the enumerative algorithm or the DNSPSO algorithm with $D = 1$.

Pseudocode: The DNSPSO Algorithm

Uniformly randomly initialize each particle in the swarm;

Specify N, w_a, c_1, c_2, k_n, p_r, p_{ns}, and initialize $pbest_i$ and $gbest$;

While FEs $\leqslant$ MaxFEs **do**

  For $i = 1$ to N

    Update the velocity OV_i and position OX_i of particle P_i using:

$$ov_{i,j}(t+1) = w_a \times ov_{i,j}(t) + c_1 \times rand1_{i,j} \times (pbest_{i,j}(t) - ox_{i,j}(t)) + c_2 \times rand2_{i,j} \times (gbest_j(t) - ox_{i,j}(t));$$

$$ox_{i,j}(t+1) = ox_{i,j}(t) + ov_{i,j}(t+1);$$

    Calculate the fitness value of particle P_i;

    FEs=FEs+1;

    % Diversity enhance mechanism *%*

    Generate a new trial particle $TP_i = (TX_i, TV_i)$ using the following diversity enhanced mechanism:

$$tx_{i,j}(t+1) = \begin{cases} ox_{i,j}(t+1), & \text{if } rand_j(0,1) \leqslant p_r, \\ ox_{i,j}(t), & \text{otherwise;} \end{cases}$$

$$tv_{i,j}(t+1) = ov_{i,j}(t+1);$$

    Calculate the fitness value of TP_i;

    Select a better fitness value between P_i and TP_i as the new P_i, i.e.,

$$P_i = \begin{cases} TP_i, & \text{if } f_a(TP_i) \leqslant f_a(P_i), \\ P_i, & \text{otherwise;} \end{cases}$$

    Update $pbest_i$ and $gbest$;

  End

  For $i = 1$ to N

    % Neighborhood search strategy*%*

    If $rand(0,1) \leqslant p_{ns}$

      Generate a trial particle $L_i = (LX_i, LV_i)$ using the local neighborhood search (LNS) strategy:

$$LX_i = r_1 \times OX_i + r_2 \times pbest_i + r_3 \times (OX_c - OX_d);$$

$$LV_i = OV_i;$$

      Generate a trial particle $G_i = (GX_i, GV_i)$ using the global neighborhood search (GNS) strategy:

$$GX_i = r_4 \times OX_i + r_5 \times gbest + r_6 \times (OX_e - OX_f);$$

$$GV_i = OV_i;$$

      Calculate the fitness values of L_i and G_i;

      FEs=FEs+2;

      Select a better fitness value among P_i, L_i and G_i as the new P_i;

    End

    Update $pbest_i$ and $gbest$;

  End

End

Table 1: ARL and ATS values computed using the Markov chain model versus those values obtained using the Monte Carlo simulation ($m = 201$, $n \in \{1, 3\}$, and $\delta \in \{0, 0.5, 1.5, 2.5\}$).

Scenarios	δ	ATEWMA $\bar{X}$		VSI-ATEWMA $\bar{X}$	
		Markov Chain	Monte Carlo	Markov Chain	Monte Carlo
Zero-state	$n = 1$				
		$H^+ = 0.6346, \lambda = 0.0979, k = 8.8393, W^+ = -0.0315$			
	0	370	370.64	369.45	371.46
	0.5	24.60	24.63	11.23	11.30
	1.5	4.68	4.69	1.59	1.59
	2.5	2.51	2.52	0.77	0.77
	$n = 3$				
		$H^+ = 0.6424, \lambda = 0.0768, k = 3.9556, W^+ = -0.0250$			
	0	370	370.43	369.15	369.02
	0.5	12.44	12.44	4.69	4.68
	1.5	2.17	2.17	0.66	0.66
	2.5	1.08	1.08	0.32	0.32
Steady-state	$n = 1$				
		$H^+ = 0.6802, \lambda = 0.1071, k = 8.6228, W^+ = -0.0430$			
	0	370	369.64	369.49	371.04
	0.5	25.12	24.94	14.58	14.43
	1.5	4.74	4.65	2.80	2.75
	2.5	2.54	2.49	1.48	1.48
	$n = 3$				
		$H^+ = 0.5705, \lambda = 0.0617, k = 3.9254, W^+ = -0.0255$			
	0	370	369.82	370.16	371.28
	0.5	12.98	12.71	7.79	7.31
	1.5	2.16	2.14	1.41	1.39
	2.5	1.08	1.08	0.79	0.83

Table 2: Optimal parameters of the recommended upper-sided ATEWMA $\bar{X}$ scheme, the conventional AEWMA $\bar{X}$ scheme, and the upper-sided TEWMA $\bar{X}$ scheme (Zero-state case, $\mathrm{ARL}_0 = 370,\ n \in \{1, 3\}$).

δ_S	δ_L	ATEWMA $\bar{X}$			AEWMA $\bar{X}$			δ_T	TEWMA $\bar{X}$	
		H^+	λ	k	H'	λ'	k'		r	h^+
					$n = 1$					
0.25	1.00	0.4000	0.0534	6.1642	0.5246	0.0767	5.3905	0.25	0.0101	0.0711
0.50	1.00	0.6054	0.0919	7.1278	0.5125	0.0739	6.9808	0.50	0.0102	0.0715
0.75	1.00	0.4928	0.0701	8.1906	0.5679	0.0870	4.3315	0.75	0.0735	0.5109
0.25	2.00	0.5649	0.0839	7.4515	0.7634	0.1395	3.9524	1.00	0.1094	0.6900
0.50	2.00	0.6046	0.0918	6.8834	0.7632	0.1395	3.9527	1.25	0.1509	0.8773
0.75	2.00	0.6346	0.0979	8.8393	0.7481	0.1353	8.1341	1.50	0.2043	1.1003
0.25	3.00	0.6947	0.0974	4.2221	0.3588	0.0258	2.7698	2.00	0.3698	1.7263
0.50	3.00	0.7109	0.1045	4.3796	0.4427	0.0353	2.7045	2.50	0.4959	2.1783
0.75	3.00	0.7418	0.1125	4.4691	0.7481	0.1212	2.8638	3.00	0.6547	2.7502
					$n = 3$					
0.25	1.00	0.5729	0.0855	6.8447	0.7473	0.1351	9.9843	0.25	0.0101	0.0711
0.50	1.00	0.5617	0.0833	7.8306	0.7134	0.1253	6.4174	0.50	0.0885	0.5894
0.75	1.00	0.7970	0.1327	6.9773	0.7844	0.1452	3.6739	0.75	0.1730	0.9715
0.25	2.00	0.4553	0.0420	3.9207	0.4508	0.0457	2.8025	1.00	0.2647	1.3365
0.50	2.00	0.6660	0.0845	4.0193	0.6822	0.0891	2.6678	1.25	0.3941	1.8139
0.75	2.00	0.6424	0.0768	3.9556	0.6529	0.0838	2.6929	1.50	0.5129	2.2390
0.25	3.00	0.3432	0.0426	5.0539	0.4580	0.0591	3.2324	2.00	0.7578	3.1319
0.50	3.00	0.7199	0.1043	4.2893	0.7336	0.1277	3.2731	2.50	0.9164	3.7448
0.75	3.00	0.7600	0.1191	4.6588	0.7017	0.1190	3.2921	3.00	0.9814	4.0057

Table 3: Optimal parameters of the recommended upper-sided ATEWMA $\bar{X}$ scheme, the conventional AEWMA $\bar{X}$ scheme, and the upper-sided TEWMA $\bar{X}$ scheme (Steady-state case, $\mathrm{ARL}_0 = 370,\ n \in \{1, 3\}$).

δ_S	δ_L	ATEWMA $\bar{X}$			AEWMA $\bar{X}$			δ_T	TEWMA $\bar{X}$	
		H^+	λ	k	H'	λ'	k'		r	h^+
					$n = 1$					
0.25	1.00	0.5559	0.0819	7.7593	0.6613	0.1104	6.0966	0.25	0.0335	0.2752
0.50	1.00	0.5173	0.0744	6.1899	0.5521	0.0826	6.6094	0.50	0.0588	0.4322
0.75	1.00	0.6367	0.0981	9.2143	0.5944	0.0930	7.3121	0.75	0.0909	0.6023
0.25	2.00	0.7013	0.1116	8.5037	0.6335	0.1024	3.6737	1.00	0.1304	0.7881
0.50	2.00	0.6838	0.1079	8.2647	0.6914	0.1187	6.2633	1.25	0.1761	0.9856
0.75	2.00	0.6802	0.1071	8.6228	0.6525	0.1081	4.4318	1.50	0.2251	1.1841
0.25	3.00	0.7207	0.1034	4.2555	0.6222	0.0870	2.8613	2.00	0.3481	1.6479
0.50	3.00	0.6019	0.0833	4.4195	0.6377	0.1018	3.3457	2.50	0.5025	2.2027
0.75	3.00	0.6923	0.0974	4.2464	0.7118	0.1140	2.9462	3.00	0.6519	2.7402
					$n = 3$					
0.25	1.00	0.5548	0.0800	5.1039	0.6801	0.1156	5.0431	0.25	0.0519	0.3917
0.50	1.00	0.7201	0.1156	8.4973	0.7129	0.1247	6.8712	0.50	0.1073	0.6808
0.75	1.00	0.7692	0.1263	8.3073	0.7815	0.1447	8.7480	0.75	0.1823	1.0111
0.25	2.00	0.6419	0.0847	4.1518	0.5532	0.0668	2.7959	1.00	0.2781	1.3885
0.50	2.00	0.7442	0.1026	4.0843	0.7664	0.1228	2.8047	1.25	0.3937	1.8133
0.75	2.00	0.5705	0.0617	3.9254	0.7872	0.1049	2.5600	1.50	0.5291	2.2975
0.25	3.00	0.6516	0.1006	5.5516	0.5407	0.0780	3.3726	2.00	0.7772	3.2054
0.50	3.00	0.7868	0.1295	5.5469	0.6726	0.1095	3.2134	2.50	0.9336	3.8130
0.75	3.00	0.7498	0.1204	5.1788	0.7423	0.1231	2.9635	3.00	0.9913	4.0460

Table 4: Zero-state ARL comparisons between the suggested upper-sided ATEWMA $\bar{X}$ scheme and the conventional AEWMA $\bar{X}$ scheme for $\mathrm{ARL}_0 = 370$ and $n \in \{1, 3\}$.

δ_S	δ_L	Schemes	δ									
			0.25	0.50	0.75	1.00	1.25	1.50	1.75	2.00	2.50	3.00
						$n = 1$						
0.25	1.00	AEWMA	81.57	27.06	14.78	10.03	7.60	6.13	5.16	4.46	3.55	2.97
		ATEWMA	60.05	22.98	12.88	8.63	6.40	5.05	4.16	3.54	2.72	2.19
0.50	1.00	AEWMA	82.31	26.56	14.17	9.44	7.02	5.57	4.61	3.93	3.03	2.46
		ATEWMA	67.72	24.37	12.89	8.34	6.05	4.72	3.86	3.28	2.54	2.12
0.75	1.00	AEWMA	85.00	27.53	14.73	9.88	7.43	5.96	5.00	4.31	3.39	2.78
		ATEWMA	63.36	23.48	12.81	8.46	6.21	4.88	4.01	3.42	2.66	2.21
0.25	2.00	AEWMA	102.57	31.03	15.16	9.59	6.95	5.46	4.50	3.84	2.97	2.39
		ATEWMA	65.98	23.93	12.79	8.33	6.07	4.75	3.89	3.31	2.57	2.14
0.50	2.00	AEWMA	102.55	31.02	15.16	9.59	6.95	5.46	4.51	3.84	2.97	2.39
		ATEWMA	67.71	24.37	12.89	8.35	6.06	4.72	3.87	3.28	2.55	2.12
0.75	2.00	AEWMA	100.83	30.61	15.07	9.58	6.97	5.49	4.55	3.89	3.06	2.54
		ATEWMA	68.83	24.60	12.91	8.31	6.01	4.68	3.82	3.24	2.51	2.09
0.25	3.00	AEWMA	114.41	40.00	22.58	15.24	11.11	8.40	6.46	5.00	3.06	2.01
		ATEWMA	82.37	28.50	14.41	9.04	6.40	4.87	3.88	3.20	2.29	1.74
0.50	3.00	AEWMA	130.21	41.37	22.16	14.63	10.58	7.98	6.15	4.79	2.98	1.98
		ATEWMA	79.64	27.66	14.01	8.80	6.24	4.77	3.82	3.15	2.29	1.75
0.75	3.00	AEWMA	117.09	34.72	16.58	10.35	7.40	5.71	4.60	3.80	2.72	2.01
		ATEWMA	79.54	27.60	13.91	8.71	6.16	4.70	3.77	3.12	2.28	1.76
						$n = 3$						
0.25	1.00	AEWMA	39.70	11.94	6.62	4.60	3.57	2.94	2.52	2.23	1.91	1.63
		ATEWMA	30.05	10.32	5.76	3.94	3.01	2.47	2.12	1.88	1.49	1.19
0.50	1.00	AEWMA	38.61	11.90	6.69	4.67	3.63	3.00	2.57	2.27	1.95	1.69
		ATEWMA	29.89	10.32	5.78	3.96	3.02	2.48	2.13	1.88	1.50	1.19
0.75	1.00	AEWMA	41.27	12.06	6.58	4.52	3.44	2.76	2.27	1.88	1.36	1.11
		ATEWMA	33.54	10.52	5.60	3.75	2.83	2.31	1.97	1.72	1.34	1.10
0.25	2.00	AEWMA	42.57	15.15	8.70	5.72	3.93	2.76	2.00	1.54	1.13	1.02
		ATEWMA	40.45	13.72	7.35	4.64	3.15	2.24	1.69	1.36	1.07	1.01
0.50	2.00	AEWMA	51.63	14.64	7.83	5.08	3.54	2.55	1.91	1.50	1.12	1.02
		ATEWMA	38.72	12.07	6.36	4.09	2.90	2.17	1.69	1.38	1.09	1.01
0.75	2.00	AEWMA	49.47	14.48	7.84	5.12	3.57	2.58	1.92	1.51	1.12	1.02
		ATEWMA	39.87	12.44	6.54	4.19	2.93	2.17	1.68	1.37	1.08	1.01
0.25	3.00	AEWMA	34.47	12.80	7.67	5.38	4.01	3.06	2.34	1.81	1.24	1.05
		ATEWMA	28.44	10.85	6.28	4.31	3.22	2.51	2.01	1.63	1.19	1.04
0.50	3.00	AEWMA	40.52	12.16	6.71	4.60	3.46	2.72	2.18	1.77	1.25	1.05
		ATEWMA	35.98	11.25	5.96	3.90	2.82	2.16	1.71	1.41	1.11	1.02
0.75	3.00	AEWMA	39.41	12.12	6.77	4.66	3.52	2.77	2.21	1.79	1.26	1.06
		ATEWMA	34.50	10.79	5.72	3.78	2.78	2.17	1.75	1.47	1.14	1.03

Table 5: Steady-state ARL comparisons between the suggested upper-sided ATEWMA $\bar{X}$ scheme and the conventional AEWMA $\bar{X}$ scheme for $\mathrm{ARL}_0 = 370$ and $n \in \{1, 3\}$.

δ_S	δ_L	Schemes	δ									
			0.25	0.50	0.75	1.00	1.25	1.50	1.75	2.00	2.50	3.00
						$n = 1$						
0.25	1.00	AEWMA	92.01	28.53	14.64	9.60	7.13	5.69	4.75	4.10	3.24	2.71
		ATEWMA	65.78	24.17	13.09	8.62	6.32	4.96	4.08	3.47	2.69	2.22
0.50	1.00	AEWMA	82.81	27.06	14.67	9.94	7.52	6.07	5.11	4.43	3.53	2.96
		ATEWMA	64.54	24.01	13.16	8.72	6.42	5.04	4.15	3.52	2.69	2.17
0.75	1.00	AEWMA	86.23	27.54	14.61	9.78	7.35	5.91	4.96	4.29	3.41	2.86
		ATEWMA	68.81	24.74	13.08	8.48	6.16	4.81	3.94	3.34	2.59	2.15
0.25	2.00	AEWMA	90.33	28.27	14.68	9.68	7.21	5.74	4.77	4.07	3.10	2.43
		ATEWMA	71.30	25.31	13.15	8.42	6.07	4.72	3.85	3.26	2.52	2.09
0.50	2.00	AEWMA	94.73	29.07	14.70	9.55	7.05	5.60	4.67	4.02	3.18	2.66
		ATEWMA	70.66	25.16	13.13	8.43	6.09	4.74	3.87	3.28	2.54	2.10
0.75	2.00	AEWMA	91.27	28.40	14.63	9.62	7.15	5.71	4.77	4.10	3.22	2.65
		ATEWMA	70.50	25.12	13.12	8.43	6.10	4.74	3.88	3.29	2.54	2.10
0.25	3.00	AEWMA	105.89	32.17	16.30	10.57	7.71	5.98	4.81	3.95	2.76	2.00
		ATEWMA	82.26	28.42	14.35	8.99	6.36	4.83	3.85	3.16	2.26	1.71
0.50	3.00	AEWMA	92.60	28.80	14.86	9.76	7.23	5.72	4.72	3.98	2.96	2.26
		ATEWMA	74.38	26.45	13.90	8.95	6.43	4.94	3.96	3.26	2.34	1.77
0.75	3.00	AEWMA	108.68	32.43	15.85	10.05	7.26	5.63	4.55	3.77	2.70	2.01
		ATEWMA	81.35	28.21	14.34	9.04	6.41	4.88	3.88	3.18	2.27	1.72
						$n = 3$						
0.25	1.00	AEWMA	37.15	11.78	6.74	4.76	3.71	3.07	2.63	2.30	1.80	1.40
		ATEWMA	30.62	10.72	6.02	4.08	3.03	2.37	1.91	1.58	1.18	1.04
0.50	1.00	AEWMA	38.12	11.78	6.66	4.67	3.64	3.01	2.59	2.29	1.89	1.63
		ATEWMA	32.17	10.49	5.73	3.88	2.95	2.40	2.05	1.80	1.46	1.22
0.75	1.00	AEWMA	40.38	11.85	6.52	4.53	3.51	2.89	2.48	2.20	1.82	1.57
		ATEWMA	32.93	10.52	5.68	3.83	2.90	2.36	2.01	1.77	1.43	1.19
0.25	2.00	AEWMA	42.56	13.96	7.87	5.19	3.62	2.61	1.95	1.53	1.13	1.02
		ATEWMA	36.15	11.64	6.22	4.04	2.87	2.15	1.68	1.38	1.09	1.01
0.50	2.00	AEWMA	47.21	13.11	6.96	4.58	3.28	2.46	1.90	1.52	1.14	1.02
		ATEWMA	38.54	11.76	6.14	3.95	2.80	2.11	1.66	1.37	1.09	1.01
0.75	2.00	AEWMA	63.04	15.58	7.84	4.94	3.39	2.44	1.83	1.46	1.11	1.02
		ATEWMA	40.20	12.98	6.87	4.34	2.98	2.16	1.66	1.35	1.08	1.01
0.25	3.00	AEWMA	34.72	12.23	7.24	5.08	3.83	2.96	2.32	1.84	1.27	1.06
		ATEWMA	31.42	10.53	5.82	3.94	2.96	2.36	1.94	1.63	1.23	1.05
0.50	3.00	AEWMA	38.45	12.06	6.81	4.68	3.49	2.70	2.12	1.71	1.22	1.05
		ATEWMA	33.43	10.58	5.67	3.79	2.84	2.26	1.87	1.58	1.22	1.05
0.75	3.00	AEWMA	43.01	12.50	6.79	4.55	3.32	2.52	1.97	1.58	1.18	1.04
		ATEWMA	33.13	10.60	5.71	3.82	2.84	2.24	1.84	1.54	1.17	1.03

Table 6: Optimal parameters of the recommended upper-sided VSI-ATEWMA $\bar{X}$ scheme, the conventional VSI-AEWMA $\bar{X}$ scheme, and the upper-sided VSI- TEWMA $\bar{X}$ scheme (Zero-state case, $\mathrm{ATS}_0 = 370,$ and $n \in \{1, 3\}$).

δ_S	δ_L	VSI-ATEWMA $\bar{X}$				VSI-AEWMA $\bar{X}$					δ_T	VSI-TEWMA $\bar{X}$		
		H^+	λ	k	W^+	H'	λ'	k'	w' $(d_0 = d_L)$	w' $(d_0 = d_S)$		r	h^+	w^+
							$n = 1$							
0.25	1.00	0.4000	0.0534	6.1642	-0.0234	0.5246	0.0767	5.3905	0.2481	0.2477	0.25	0.0101	0.0711	-0.0549
0.50	1.00	0.6054	0.0919	7.1278	-0.0313	0.5125	0.0739	6.9808	0.2441	0.2405	0.50	0.0102	0.0715	-0.0574
0.75	1.00	0.4928	0.0701	8.1906	-0.0307	0.5679	0.0870	4.3315	0.2455	0.2422	0.75	0.0735	0.5109	-0.0316
0.25	2.00	0.5649	0.0839	7.4515	-0.0326	0.7634	0.1395	3.9524	0.2300	0.2371	1.00	0.1094	0.6900	-0.0315
0.50	2.00	0.6046	0.0918	6.8834	-0.0276	0.7632	0.1395	3.9527	0.2336	0.2307	1.25	0.1509	0.8773	-0.0442
0.75	2.00	0.6346	0.0979	8.8393	-0.0315	0.7481	0.1353	8.1341	0.2328	0.2381	1.50	0.2043	1.1003	-0.0563
0.25	3.00	0.6947	0.0974	4.2221	-0.0319	0.3588	0.0258	2.7698	0.2161	0.2149	2.00	0.3698	1.7263	-0.1064
0.50	3.00	0.7109	0.1045	4.3796	-0.0332	0.4427	0.0353	2.7045	0.2065	0.2040	2.50	0.4959	2.1783	-0.1623
0.75	3.00	0.7418	0.1125	4.4691	-0.0400	0.7481	0.1212	2.8638	0.2235	0.2258	3.00	0.6547	2.7502	-0.2320
							$n = 3$							
0.25	1.00	0.5729	0.0855	6.8447	-0.0347	0.7473	0.1351	9.9843	0.2297	0.2385	0.25	0.0101	0.0711	-0.0559
0.50	1.00	0.5617	0.0833	7.8306	-0.0328	0.7134	0.1253	6.4174	0.2316	0.2289	0.50	0.0885	0.5894	-0.0396
0.75	1.00	0.7970	0.1327	6.9773	-0.0318	0.7844	0.1452	3.6739	0.2301	0.2367	0.75	0.1730	0.9715	-0.0528
0.25	2.00	0.4553	0.0420	3.9207	-0.0150	0.4508	0.0457	2.8025	0.2224	0.2234	1.00	0.2647	1.3365	-0.0750
0.50	2.00	0.6660	0.0845	4.0193	-0.0233	0.6822	0.0891	2.6678	0.2138	0.2170	1.25	0.3941	1.8139	-0.1064
0.75	2.00	0.6424	0.0768	3.9556	-0.0250	0.6529	0.0838	2.6929	0.2188	0.2101	1.50	0.5129	2.2390	-0.1546
0.25	3.00	0.3432	0.0426	5.0539	-0.0258	0.4580	0.0591	3.2324	0.2448	0.2484	2.00	0.7578	3.1319	-0.2951
0.50	3.00	0.7199	0.1043	4.2893	-0.0358	0.7336	0.1277	3.2731	0.2316	0.2319	2.50	0.9164	3.7448	-0.4935
0.75	3.00	0.7600	0.1191	4.6588	-0.0342	0.7017	0.1190	3.2921	0.2308	0.2293	3.00	0.9814	4.0057	-0.6113

Table 7: Optimal parameters of the recommended upper-sided VSI-ATEWMA $\bar{X}$ scheme, the conventional VSI-AEWMA $\bar{X}$ scheme, and the upper-sided VSI- TEWMA $\bar{X}$ scheme (Steady-state case, $\mathrm{AATS}_0 = 370$, and $n \in \{1, 3\}$).

δ_S	δ_L	VSI-ATEWMA $\bar{X}$				VSI-AEWMA $\bar{X}$				δ_T	VSI-TEWMA $\bar{X}$		
		H^+	λ	k	W^+	H'	λ'	k'	w'		r	h^+	w^+
						$n = 1$							
0.25	1.00	0.5559	0.0819	7.7593	-0.0400	0.6613	0.1104	6.0966	0.2313	0.25	0.0335	0.2752	-0.0420
0.50	1.00	0.5173	0.0744	6.1899	-0.0468	0.5521	0.0826	6.6094	0.2311	0.50	0.0588	0.4322	-0.0420
0.75	1.00	0.6367	0.0981	9.2143	-0.0453	0.5944	0.0930	7.3121	0.2327	0.75	0.0909	0.6023	-0.0413
0.25	2.00	0.7013	0.1116	8.5037	-0.0517	0.6335	0.1024	3.6737	0.2367	1.00	0.1304	0.7881	-0.0432
0.50	2.00	0.6838	0.1079	8.2647	-0.0433	0.6914	0.1187	6.2633	0.2307	1.25	0.1761	0.9856	-0.0580
0.75	2.00	0.6802	0.1071	8.6228	-0.0430	0.6525	0.1081	4.4318	0.2362	1.50	0.2251	1.1841	-0.0724
0.25	3.00	0.7207	0.1034	4.2555	-0.0393	0.6222	0.0870	2.8613	0.2251	2.00	0.3481	1.6479	-0.1047
0.50	3.00	0.6019	0.0833	4.4195	-0.0349	0.6377	0.1018	3.3457	0.2316	2.50	0.5025	2.2027	-0.1674
0.75	3.00	0.6923	0.0974	4.2464	-0.0370	0.7118	0.1140	2.9462	0.2285	3.00	0.6519	2.7402	-0.2341
						$n = 3$							
0.25	1.00	0.5548	0.0800	5.1039	-0.0424	0.6801	0.1156	5.0431	0.2294	0.25	0.0519	0.3917	-0.0428
0.50	1.00	0.7201	0.1156	8.4973	-0.0356	0.7129	0.1247	6.8712	0.2323	0.50	0.1073	0.6808	-0.0461
0.75	1.00	0.7692	0.1263	8.3073	-0.0467	0.7815	0.1447	8.7480	0.2349	0.75	0.1823	1.0111	-0.0634
0.25	2.00	0.6419	0.0847	4.1518	-0.0356	0.5532	0.0668	2.7959	0.2218	1.00	0.2781	1.3885	-0.0816
0.50	2.00	0.7442	0.1026	4.0843	-0.0341	0.7664	0.1228	2.8047	0.2203	1.25	0.3937	1.8133	-0.1236
0.75	2.00	0.5705	0.0617	3.9254	-0.0255	0.7872	0.1049	2.5600	0.2010	1.50	0.5291	2.2975	-0.1770
0.25	3.00	0.6516	0.1006	5.5516	-0.0459	0.5407	0.0780	3.3726	0.2314	2.00	0.7772	3.2054	-0.3394
0.50	3.00	0.7868	0.1295	5.5469	-0.0493	0.6726	0.1095	3.2134	0.2372	2.50	0.9336	3.8130	-0.5349
0.75	3.00	0.7498	0.1204	5.1788	-0.0513	0.7423	0.1231	2.9635	0.2209	3.00	0.9913	4.0460	-0.6469

Table 8: Zero-state ATS comparisons among the proposed upper-sided VSI-ATEWMA $\bar{X}$ scheme, the proposed upper-sided FSI-ATEWMA $\bar{X}$ scheme, and the conventional VSI-AEWMA $\bar{X}$ scheme for $\mathrm{ATS}_0 = 370$ and $n \in \{1, 3\}$.

δ_S	δ_L	Schemes	δ									
			0.25	0.50	0.75	1.00	1.25	1.50	1.75	2.00	2.50	3.00
						$n = 1$						
0.25	1.00	FSI-ATEWMA	60.05	22.98	12.88	8.63	6.40	5.05	4.16	3.54	2.72	2.19
		VSI-AEWMA($d_0 = d_L$)	66.69	18.59	9.98	6.91	5.35	4.42	3.79	3.35	2.76	2.42
		VSI-AEWMA($d_0 = d_S$)	65.29	17.19	8.58	5.51	3.95	3.02	2.39	1.95	1.36	1.02
		VSI-ATEWMA	34.18	10.06	5.06	3.17	2.22	1.68	1.34	1.11	0.83	0.66
0.50	1.00	FSI-ATEWMA	67.72	24.37	12.89	8.34	6.05	4.72	3.86	3.28	2.54	2.12
		VSI-AEWMA($d_0 = d_L$)	65.69	18.52	10.02	6.95	5.39	4.45	3.82	3.37	2.78	2.44
		VSI-AEWMA($d_0 = d_S$)	64.29	17.12	8.62	5.55	3.99	3.05	2.42	1.97	1.38	1.04
		VSI-ATEWMA	41.64	11.17	5.24	3.16	2.17	1.61	1.27	1.04	0.78	0.64
0.75	1.00	FSI-ATEWMA	63.36	23.48	12.81	8.46	6.21	4.88	4.01	3.42	2.66	2.21
		VSI-AEWMA($d_0 = d_L$)	70.50	18.95	9.89	6.77	5.22	4.30	3.69	3.25	2.69	2.35
		VSI-AEWMA($d_0 = d_S$)	69.10	17.55	8.49	5.37	3.82	2.90	2.29	1.85	1.29	0.95
		VSI-ATEWMA	37.23	10.47	5.11	3.15	2.19	1.64	1.30	1.08	0.81	0.67
0.25	2.00	FSI-ATEWMA	65.98	23.93	12.79	8.33	6.07	4.75	3.89	3.31	2.57	2.14
		VSI-AEWMA($d_0 = d_L$)	88.03	21.44	9.81	6.32	4.76	3.88	3.32	2.93	2.45	2.18
		VSI-AEWMA($d_0 = d_S$)	86.63	20.04	8.41	4.92	3.36	2.48	1.92	1.53	1.05	0.78
		VSI-ATEWMA	40.02	10.82	5.13	3.11	2.14	1.60	1.26	1.04	0.79	0.65
0.50	2.00	FSI-ATEWMA	67.71	24.37	12.89	8.35	6.06	4.72	3.87	3.28	2.55	2.12
		VSI-AEWMA($d_0 = d_L$)	88.01	21.44	9.81	6.32	4.76	3.88	3.32	2.93	2.45	2.18
		VSI-AEWMA($d_0 = d_S$)	86.61	20.04	8.41	4.92	3.36	2.48	1.92	1.53	1.05	0.78
		VSI-ATEWMA	41.60	11.17	5.24	3.16	2.17	1.61	1.27	1.04	0.78	0.64
0.75	2.00	FSI-ATEWMA	68.83	24.60	12.91	8.31	6.01	4.68	3.82	3.24	2.51	2.09
		VSI-AEWMA($d_0 = d_L$)	86.18	21.10	9.77	6.33	4.78	3.90	3.34	2.96	2.48	2.22
		VSI-AEWMA($d_0 = d_S$)	84.78	19.70	8.37	4.93	3.38	2.50	1.94	1.56	1.08	0.82
		VSI-ATEWMA	42.38	11.23	5.21	3.12	2.14	1.59	1.25	1.03	0.77	0.63
0.25	3.00	FSI-ATEWMA	82.37	28.50	14.41	9.04	6.40	4.87	3.88	3.20	2.29	1.74
		VSI-AEWMA($d_0 = d_L$)	76.02	24.96	14.58	10.24	7.84	6.30	5.21	4.39	3.29	2.60
		VSI-AEWMA($d_0 = d_S$)	74.62	23.56	13.18	8.84	6.44	4.90	3.81	2.99	1.89	1.20
		VSI-ATEWMA	49.31	12.59	5.70	3.37	2.27	1.65	1.27	1.02	0.70	0.52
0.50	3.00	FSI-ATEWMA	79.64	27.66	14.01	8.80	6.24	4.77	3.82	3.15	2.29	1.75
		VSI-AEWMA($d_0 = d_L$)	86.14	24.56	13.74	9.52	7.26	5.83	4.83	4.10	3.09	2.47
		VSI-AEWMA($d_0 = d_S$)	84.74	23.16	12.34	8.12	5.86	4.43	3.43	2.70	1.69	1.07
		VSI-ATEWMA	49.10	12.51	5.62	3.31	2.23	1.63	1.25	1.01	0.70	0.53
0.75	3.00	FSI-ATEWMA	79.54	27.60	13.91	8.71	6.16	4.70	3.77	3.12	2.28	1.76
		VSI-AEWMA($d_0 = d_L$)	97.41	22.73	10.34	6.67	5.00	4.04	3.42	2.98	2.41	2.08
		VSI-AEWMA($d_0 = d_S$)	96.01	21.33	8.94	5.27	3.60	2.64	2.02	1.58	1.01	0.68
		VSI-ATEWMA	49.27	12.52	5.57	3.26	2.19	1.60	1.24	0.99	0.70	0.53
						$n = 3$						
0.25	1.00	FSI-ATEWMA	30.05	10.32	5.76	3.94	3.01	2.47	2.12	1.88	1.49	1.19
		VSI-AEWMA($d_0 = d_L$)	28.58	7.77	4.57	3.37	2.77	2.42	2.21	2.09	1.98	1.89
		VSI-AEWMA($d_0 = d_S$)	27.18	6.37	3.17	1.97	1.37	1.02	0.81	0.69	0.58	0.49
		VSI-ATEWMA	14.29	3.98	2.01	1.28	0.94	0.75	0.64	0.56	0.45	0.36
0.50	1.00	FSI-ATEWMA	29.89	10.32	5.78	3.96	3.02	2.48	2.13	1.88	1.50	1.19
		VSI-AEWMA($d_0 = d_L$)	27.56	7.78	4.62	3.42	2.80	2.45	2.23	2.10	1.99	1.91
		VSI-AEWMA($d_0 = d_S$)	26.16	6.38	3.22	2.02	1.40	1.05	0.83	0.70	0.59	0.51
		VSI-ATEWMA	14.13	3.98	2.02	1.29	0.94	0.75	0.64	0.57	0.45	0.36
0.75	1.00	FSI-ATEWMA	33.54	10.52	5.60	3.75	2.83	2.31	1.97	1.72	1.34	1.10
		VSI-AEWMA($d_0 = d_L$)	29.97	7.81	4.53	3.33	2.72	2.36	2.14	1.98	1.81	1.73
		VSI-AEWMA($d_0 = d_S$)	28.57	6.41	3.13	1.93	1.32	0.96	0.74	0.58	0.41	0.33
		VSI-ATEWMA	17.02	4.19	2.01	1.25	0.89	0.71	0.59	0.52	0.40	0.33
0.25	2.00	FSI-ATEWMA	40.45	13.72	7.35	4.64	3.15	2.24	1.69	1.36	1.07	1.01
		VSI-AEWMA($d_0 = d_L$)	27.19	10.00	6.17	4.44	3.42	2.74	2.29	2.01	1.76	1.71
		VSI-AEWMA($d_0 = d_S$)	25.79	8.60	4.77	3.04	2.02	1.34	0.89	0.61	0.36	0.31
		VSI-ATEWMA	16.87	5.04	2.51	1.50	0.98	0.68	0.51	0.41	0.32	0.30
0.50	2.00	FSI-ATEWMA	38.72	12.07	6.36	4.09	2.90	2.17	1.69	1.38	1.09	1.01
		VSI-AEWMA($d_0 = d_L$)	32.62	9.03	5.28	3.77	2.93	2.41	2.09	1.90	1.74	1.71
		VSI-AEWMA($d_0 = d_S$)	31.22	7.63	3.88	2.37	1.53	1.01	0.69	0.50	0.34	0.31
		VSI-ATEWMA	17.65	4.61	2.23	1.35	0.91	0.66	0.51	0.41	0.33	0.30
0.75	2.00	FSI-ATEWMA	39.87	12.44	6.54	4.19	2.93	2.17	1.68	1.37	1.08	1.01
		VSI-AEWMA($d_0 = d_L$)	31.16	9.00	5.32	3.80	2.96	2.43	2.10	1.90	1.74	1.71
		VSI-AEWMA($d_0 = d_S$)	29.76	7.60	3.92	2.40	1.56	1.03	0.70	0.50	0.34	0.31
		VSI-ATEWMA	17.66	4.69	2.28	1.37	0.92	0.66	0.51	0.41	0.32	0.30
0.25	3.00	FSI-ATEWMA	28.44	10.85	6.28	4.31	3.22	2.51	2.01	1.63	1.19	1.04
		VSI-AEWMA($d_0 = d_L$)	23.94	8.79	5.50	4.06	3.22	2.67	2.28	2.03	1.78	1.71
		VSI-AEWMA($d_0 = d_S$)	22.54	7.39	4.10	2.66	1.82	1.27	0.88	0.63	0.38	0.31
		VSI-ATEWMA	12.70	4.04	2.13	1.38	0.99	0.76	0.60	0.49	0.36	0.31
0.50	3.00	FSI-ATEWMA	35.98	11.25	5.96	3.90	2.82	2.16	1.71	1.41	1.11	1.02
		VSI-AEWMA($d_0 = d_L$)	28.90	7.90	4.65	3.41	2.76	2.37	2.12	1.95	1.78	1.72
		VSI-AEWMA($d_0 = d_S$)	27.50	6.50	3.25	2.01	1.36	0.97	0.72	0.55	0.38	0.32
		VSI-ATEWMA	17.07	4.35	2.10	1.28	0.89	0.66	0.52	0.42	0.33	0.30
0.75	3.00	FSI-ATEWMA	34.50	10.79	5.72	3.78	2.78	2.17	1.75	1.47	1.14	1.03
		VSI-AEWMA($d_0 = d_L$)	27.89	7.91	4.70	3.45	2.79	2.39	2.13	1.96	1.78	1.72
		VSI-AEWMA($d_0 = d_S$)	26.49	6.51	3.30	2.05	1.39	0.99	0.73	0.56	0.38	0.32
		VSI-ATEWMA	16.85	4.20	2.02	1.24	0.87	0.66	0.53	0.44	0.34	0.31

Table 9: Steady-state ATS comparisons among the proposed upper-sided VSI-ATEWMA $\bar{X}$ scheme, the proposed upper-sided FSI-ATEWMA $\bar{X}$ scheme, and the conventional VSI-AEWMA $\bar{X}$ scheme for $\mathrm{AATS}_0 = 370$ and $n \in \{1, 3\}$.

δ_S	δ_L	Schemes	δ									
			0.25	0.50	0.75	1.00	1.25	1.50	1.75	2.00	2.50	3.00
						$n = 1$						
0.25	1.00	FSI-ATEWMA	65.78	24.17	13.09	8.62	6.32	4.96	4.08	3.47	2.69	2.22
		VSI-AEWMA	76.19	18.40	8.61	5.50	4.04	3.20	2.65	2.26	1.76	1.45
		VSI-ATEWMA	44.25	14.63	8.02	5.35	3.93	3.07	2.51	2.12	1.62	1.34
0.50	1.00	FSI-ATEWMA	64.54	24.01	13.16	8.72	6.42	5.04	4.15	3.52	2.69	2.17
		VSI-AEWMA	65.99	17.15	8.70	5.78	4.33	3.46	2.88	2.47	1.93	1.59
		VSI-ATEWMA	43.29	14.74	8.20	5.50	4.06	3.17	2.59	2.18	1.65	1.33
0.75	1.00	FSI-ATEWMA	68.81	24.74	13.08	8.48	6.16	4.81	3.94	3.34	2.59	2.15
		VSI-AEWMA	69.79	17.55	8.63	5.66	4.21	3.35	2.78	2.38	1.85	1.53
		VSI-ATEWMA	46.37	14.53	7.70	5.06	3.69	2.88	2.34	1.98	1.52	1.27
0.25	2.00	FSI-ATEWMA	71.30	25.31	13.15	8.42	6.07	4.72	3.85	3.26	2.52	2.09
		VSI-AEWMA	74.07	18.11	8.64	5.58	4.12	3.26	2.69	2.28	1.74	1.38
		VSI-ATEWMA	48.11	14.57	7.53	4.89	3.55	2.76	2.24	1.89	1.46	1.22
0.50	2.00	FSI-ATEWMA	70.66	25.16	13.13	8.43	6.09	4.74	3.87	3.28	2.54	2.10
		VSI-AEWMA	79.20	18.86	8.63	5.45	3.98	3.14	2.59	2.21	1.72	1.42
		VSI-ATEWMA	47.90	14.62	7.60	4.95	3.60	2.80	2.28	1.92	1.48	1.24
0.75	2.00	FSI-ATEWMA	70.50	25.12	13.12	8.43	6.10	4.74	3.88	3.29	2.54	2.10
		VSI-AEWMA	75.35	18.28	8.61	5.52	4.06	3.21	2.66	2.27	1.76	1.44
		VSI-ATEWMA	47.64	14.58	7.60	4.95	3.60	2.80	2.28	1.92	1.48	1.24
0.25	3.00	FSI-ATEWMA	82.26	28.42	14.35	8.99	6.36	4.83	3.85	3.16	2.26	1.71
		VSI-AEWMA	83.35	19.54	9.34	6.04	4.42	3.45	2.80	2.33	1.67	1.26
		VSI-ATEWMA	53.87	15.78	8.02	5.15	3.69	2.82	2.25	1.86	1.35	1.07
0.50	3.00	FSI-ATEWMA	74.38	26.45	13.90	8.95	6.43	4.94	3.96	3.26	2.34	1.77
		VSI-AEWMA	75.96	18.40	8.74	5.63	4.14	3.27	2.68	2.27	1.70	1.33
		VSI-ATEWMA	48.79	15.42	8.26	5.42	3.93	3.03	2.42	2.00	1.45	1.13
0.75	3.00	FSI-ATEWMA	81.35	28.21	14.34	9.04	6.41	4.88	3.88	3.18	2.27	1.72
		VSI-AEWMA	88.81	20.23	9.02	5.64	4.08	3.17	2.58	2.15	1.57	1.21
		VSI-ATEWMA	52.65	15.70	8.10	5.23	3.76	2.88	2.30	1.89	1.37	1.08
						$n = 3$						
0.25	1.00	FSI-ATEWMA	30.62	10.72	6.02	4.08	3.03	2.37	1.91	1.58	1.18	1.04
		VSI-AEWMA	25.34	6.81	3.80	2.64	2.03	1.66	1.41	1.24	1.03	0.88
		VSI-ATEWMA	18.53	6.59	3.74	2.52	1.86	1.46	1.19	1.01	0.82	0.76
0.50	1.00	FSI-ATEWMA	32.17	10.49	5.73	3.88	2.95	2.40	2.05	1.80	1.46	1.22
		VSI-AEWMA	26.26	6.78	3.74	2.59	1.99	1.62	1.39	1.23	1.05	0.95
		VSI-ATEWMA	19.44	6.13	3.39	2.29	1.73	1.41	1.21	1.09	0.95	0.85
0.75	1.00	FSI-ATEWMA	32.93	10.52	5.68	3.83	2.90	2.36	2.01	1.77	1.43	1.19
		VSI-AEWMA	28.44	6.79	3.63	2.49	1.90	1.55	1.33	1.18	1.02	0.92
		VSI-ATEWMA	19.34	5.95	3.26	2.20	1.66	1.36	1.18	1.06	0.93	0.84
0.25	2.00	FSI-ATEWMA	36.15	11.64	6.22	4.04	2.87	2.15	1.68	1.38	1.09	1.01
		VSI-AEWMA	26.21	8.08	4.61	3.10	2.23	1.66	1.28	1.04	0.81	0.75
		VSI-ATEWMA	20.43	6.78	3.73	2.43	1.74	1.33	1.08	0.92	0.79	0.75
0.50	2.00	FSI-ATEWMA	38.54	11.76	6.14	3.95	2.80	2.11	1.66	1.37	1.09	1.01
		VSI-AEWMA	31.34	7.31	3.89	2.60	1.90	1.46	1.17	0.98	0.80	0.75
		VSI-ATEWMA	21.28	6.56	3.54	2.30	1.66	1.28	1.04	0.90	0.78	0.75
0.75	2.00	FSI-ATEWMA	40.20	12.98	6.87	4.34	2.98	2.16	1.66	1.35	1.08	1.01
		VSI-AEWMA	38.08	8.20	4.27	2.78	1.97	1.47	1.16	0.96	0.79	0.74
		VSI-ATEWMA	22.41	7.79	4.27	2.73	1.90	1.41	1.11	0.94	0.79	0.76
0.25	3.00	FSI-ATEWMA	31.42	10.53	5.82	3.94	2.96	2.36	1.94	1.63	1.23	1.05
		VSI-AEWMA	22.75	7.20	4.20	2.93	2.21	1.74	1.39	1.14	0.86	0.76
		VSI-ATEWMA	18.60	6.20	3.47	2.34	1.75	1.40	1.17	1.01	0.83	0.77
0.50	3.00	FSI-ATEWMA	33.43	10.58	5.67	3.79	2.84	2.26	1.87	1.58	1.22	1.05
		VSI-AEWMA	25.97	6.98	3.89	2.67	2.00	1.56	1.26	1.06	0.83	0.76
		VSI-ATEWMA	19.55	5.94	3.24	2.17	1.63	1.31	1.11	0.98	0.83	0.76
0.75	3.00	FSI-ATEWMA	33.13	10.60	5.71	3.82	2.84	2.24	1.84	1.54	1.18	1.04
		VSI-AEWMA	28.68	7.02	3.79	2.56	1.89	1.47	1.18	0.99	0.80	0.75
		VSI-ATEWMA	19.20	6.00	3.29	2.20	1.64	1.31	1.10	0.96	0.81	0.76

Table 10: The charting statistics of the recommended upper-sided ATEWMA $\bar{X}$ scheme, the conventional AEWMA $\bar{X}$ scheme, and the upper-sided TEWMA $\bar{X}$ scheme corresponding to the zero-state and the steady-state datasets ($\mu_0 = 100$, $\sigma_0 = 3$, $n = 1$).

Zero-state case										Steady-state case									
$\delta = 0.75 \times \sigma_0$					$\delta = 2 \times \sigma_0$					$\delta = 0.75 \times \sigma_0$					$\delta = 2 \times \sigma_0$				
t	X_t	Q_t^+	Q_t	$Q_{T,t}^+$	t	X_t	Q_t^+	Q_t	$Q_{T,t}^+$	t	X_t	Q_t^+	Q_t	$Q_{T,t}^+$	t	X_t	Q_t^+	Q_t	$Q_{T,t}^+$
-	-	0	0	0	-	-	0	0	0	-	-	0	0	0	-	-	0	0	0
1.	100.68	-0.03	0.03	-0.06	1.	103.72	0.14	0.17	0.29	1.	96.84	-0.07	-0.11	-0.15	1.	102.14	0.06	0.08	0.12
2.	103.85	0.12	0.20	0.26	2.	99.28	0.06	0.11	0.09	2.	99.01	-0.14	-0.14	-0.27	2.	96.00	-0.02	-0.08	-0.06
3.	103.79	0.26	0.34	0.51	3.	104.40	0.23	0.30	0.45	3.	103.62	0.02	0.01	0.10	3.	103.19	0.10	0.05	0.21
4.	100.91	0.21	0.34	0.37	4.	105.45	0.45	0.50	0.85	4.	100.53	-0.02	0.03	-0.01	4.	99.84	0.02	0.04	0.01
5.	101.80	0.23	0.37	0.37	5.	103.33	0.52	0.58	0.93	5.	96.98	-0.09	-0.09	-0.16	5.	100.04	-0.05	0.03	-0.14
6.	103.74	0.35	0.49	0.59	6.	102.16	0.53	0.60	0.85	6.	94.93	-0.15	-0.26	-0.28	6.	95.70	-0.12	-0.12	-0.26
7.	100.84	0.29	0.46	0.43	7.	104.69	**0.67**	0.73	1.08	7.	102.66	-0.05	-0.14	-0.03	7.	105.46	0.15	0.09	0.34
8.	107.08	0.59	0.72	1.03	8.	102.00	0.65	0.72	0.96	8.	98.34	-0.12	-0.18	-0.18	8.	102.71	0.23	0.17	0.46
9.	102.35	0.60	0.73	0.95	9.	108.76	1.01	**1.02**	**1.64**	9.	96.57	-0.18	-0.28	-0.29	9.	92.75	0.13	-0.11	0.20
10.	96.60	0.47	0.48	0.62	10.	108.02	1.29	1.24	2.10	10.	95.82	-0.23	-0.40	-0.38	10.	90.87	0.04	-0.42	0.00
11.	104.52	0.61	0.62	0.88	11.	104.05	1.32	1.26	2.01	11.	106.73	0.13	-0.12	0.42	11.	106.59	0.37	-0.14	0.70
12.	101.63	0.58	0.61	0.75	12.	108.32	1.59	1.46	2.43	12.	102.47	0.20	-0.02	0.49	12.	105.37	0.58	0.07	1.08
13.	103.92	**0.67**	0.70	0.91	13.	110.07	1.93	1.72	2.97	13.	103.66	0.33	0.12	0.69	13.	103.85	**0.684**	0.20	1.17
14.	99.60	0.54	0.59	0.59	14.	106.88	2.06	1.80	3.02	14.	103.30	0.42	0.22	0.81	14.	110.34	1.17	0.55	**2.09**
15.	103.67	0.63	0.67	0.76	15.	107.16	2.19	1.88	3.10	15.	98.93	0.30	0.16	0.47	15.	106.10	1.34	**0.71**	2.25
16.	106.21	0.84	**0.86**	**1.19**	16.	108.22	2.37	1.99	3.29	16.	103.33	0.40	0.26	0.64	16.	98.46	1.13	0.58	1.59
17.	98.92	0.70	0.70	0.80	17.	107.14	2.47	2.05	3.31	17.	105.74	0.63	0.44	1.08	17.	108.78	1.47	0.83	2.20
18.	100.27	0.58	0.62	0.53	18.	101.88	2.27	1.85	2.71	18.	98.00	0.49	0.32	0.68	18.	101.99	1.36	0.81	1.81
19.	98.42	0.45	0.46	0.28	19.	105.93	2.31	1.87	2.71	19.	101.34	0.45	0.34	0.55	19.	104.23	1.40	0.88	1.79
20.	103.09	0.51	0.54	0.45	20.	112.23	2.70	2.17	3.44	20.	102.95	0.51	0.41	0.65	20.	106.00	1.54	1.00	2.01
21.	109.36	0.92	0.89	1.31	21.	108.07	2.82	2.24	3.54	21.	101.24	0.46	0.41	0.51	21.	106.00	1.67	1.11	2.17
22.	105.92	1.09	1.03	1.59	22.	109.13	2.99	2.35	3.74	22.	106.74	**0.75**	0.61	1.11	22.	108.07	1.91	1.28	2.57
23.	100.44	0.94	0.91	1.18	23.	109.17	3.14	2.44	3.91	23.	101.58	0.69	0.60	0.91	23.	104.26	1.90	1.29	2.38
24.	98.77	0.78	0.73	0.80	24.	107.64	3.19	2.46	3.86	24.	101.88	0.66	0.60	0.79	24.	107.65	2.09	1.43	2.68
25.	101.08	0.70	0.68	0.62	25.	105.29	3.11	2.36	3.55	25.	106.79	0.93	**0.78**	**1.33**	25.	101.73	1.90	1.34	2.14

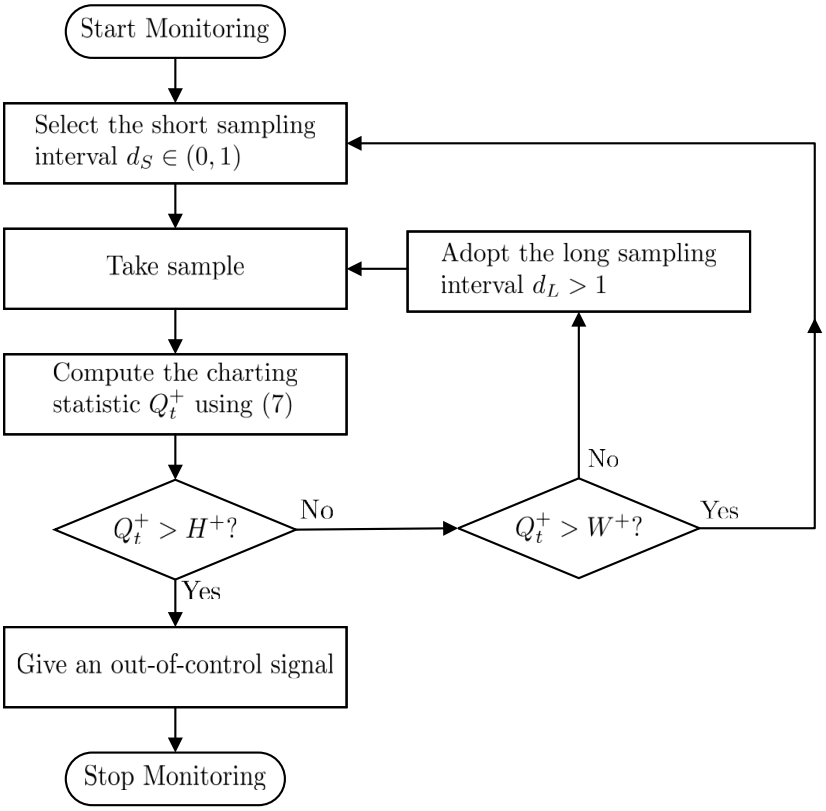

Figure 1: The flowchart for the VSI strategy used in the proposed upper-sided ATEWMA $\bar{X}$ scheme.

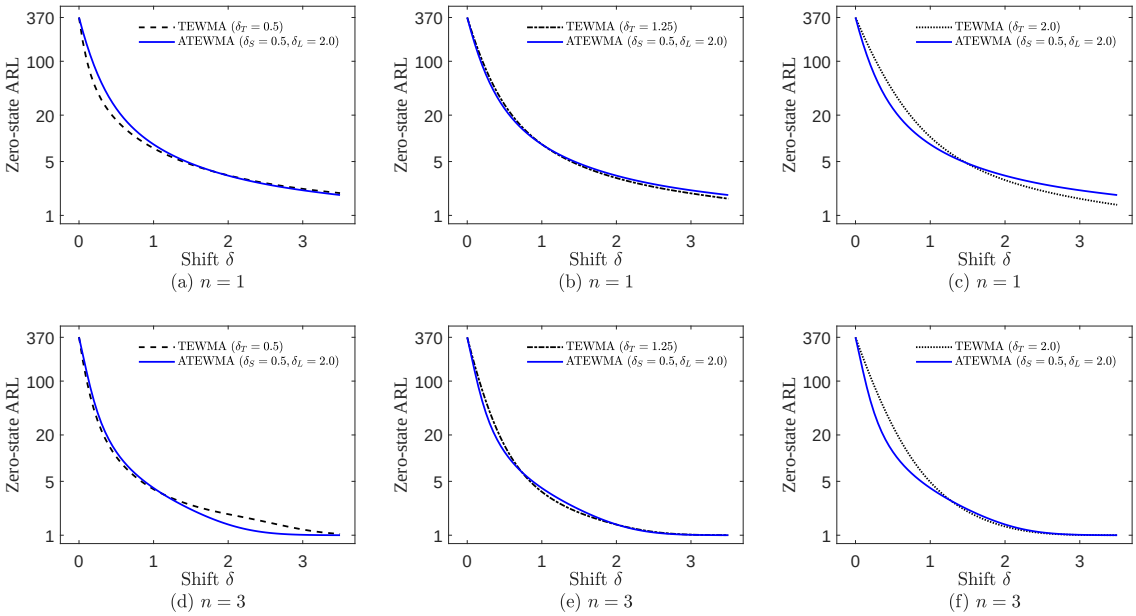

Figure 2: Zero-state ARL comparisons between the proposed upper-sided ATEWMA $\bar{X}$ scheme and the upper-sided TEWMA $\bar{X}$ scheme for $\mathrm{ARL}_0 = 370$ and $n \in \{1, 3\}$.

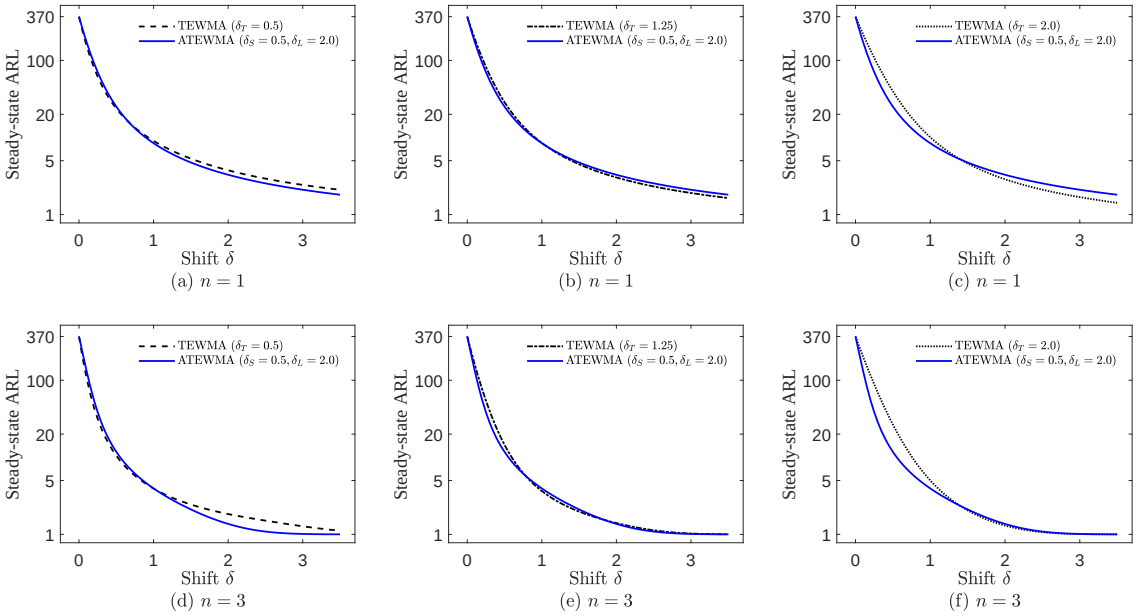

Figure 3: Steady-state ARL comparisons between the proposed upper-sided ATEWMA $\bar{X}$ scheme and the upper-sided TEWMA $\bar{X}$ scheme for $\mathrm{ARL}_0 = 370$ and $n \in \{1, 3\}$.

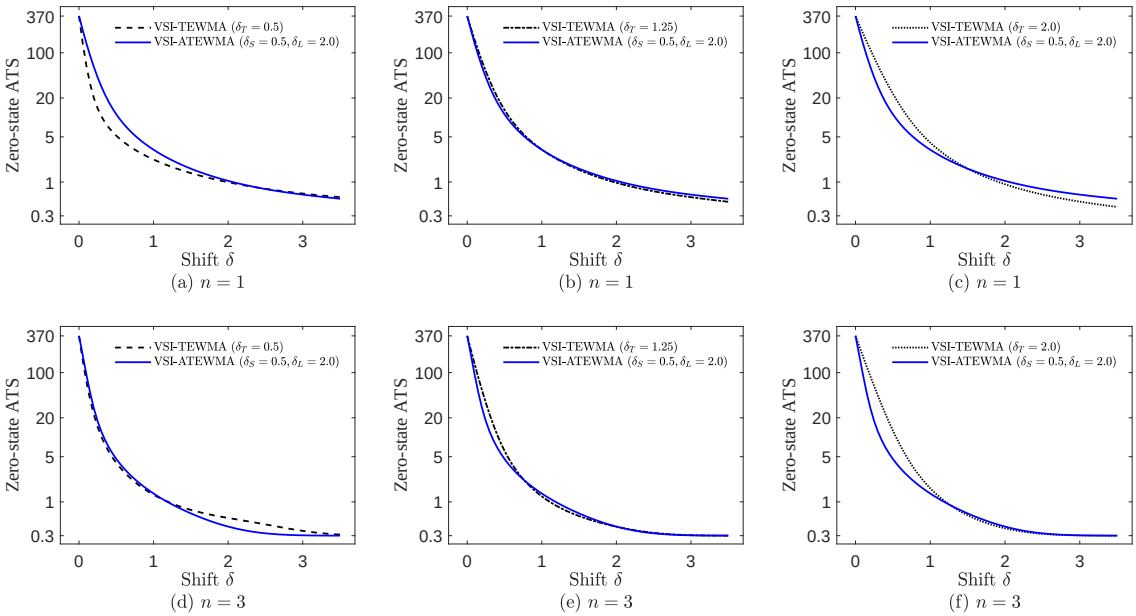

Figure 4: Zero-state ATS comparisons between the proposed upper-sided VSI-ATEWMA $\bar{X}$ scheme and the upper-sided VSI- TEWMA $\bar{X}$ scheme for $\mathrm{ATS}_0 = 370$ and $n \in \{1, 3\}$.

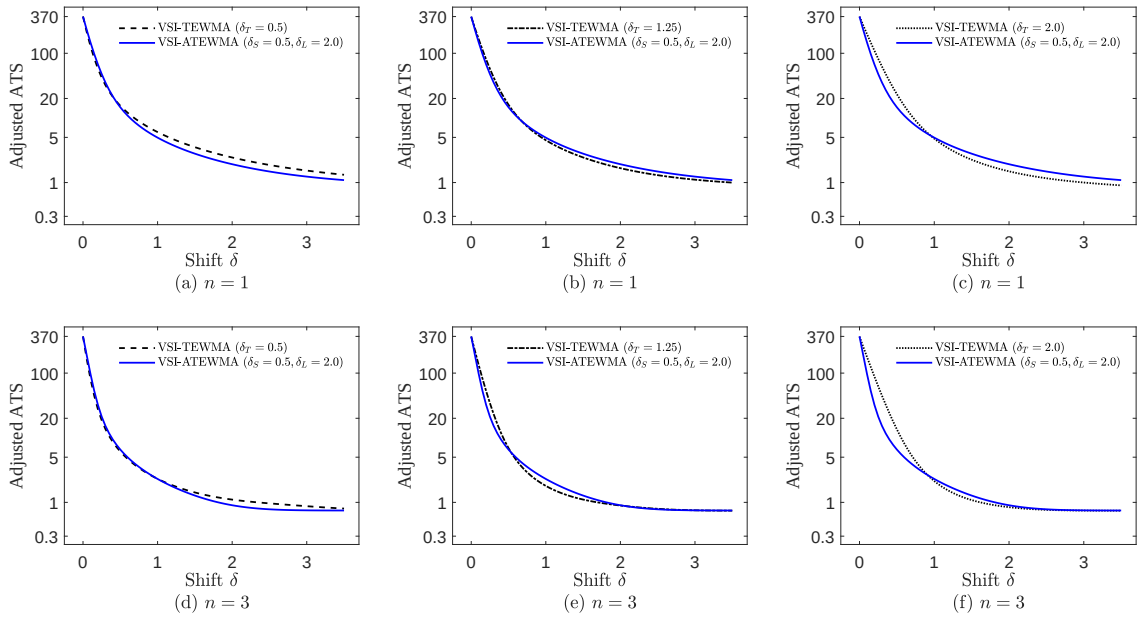

Figure 5: Adjusted ATS comparisons between the proposed upper-sided VSI-ATEWMA $\bar{X}$ scheme and the upper-sided VSI- TEWMA $\bar{X}$ scheme for $\mathrm{AATS}_0 = 370$ and $n \in \{1, 3\}$.

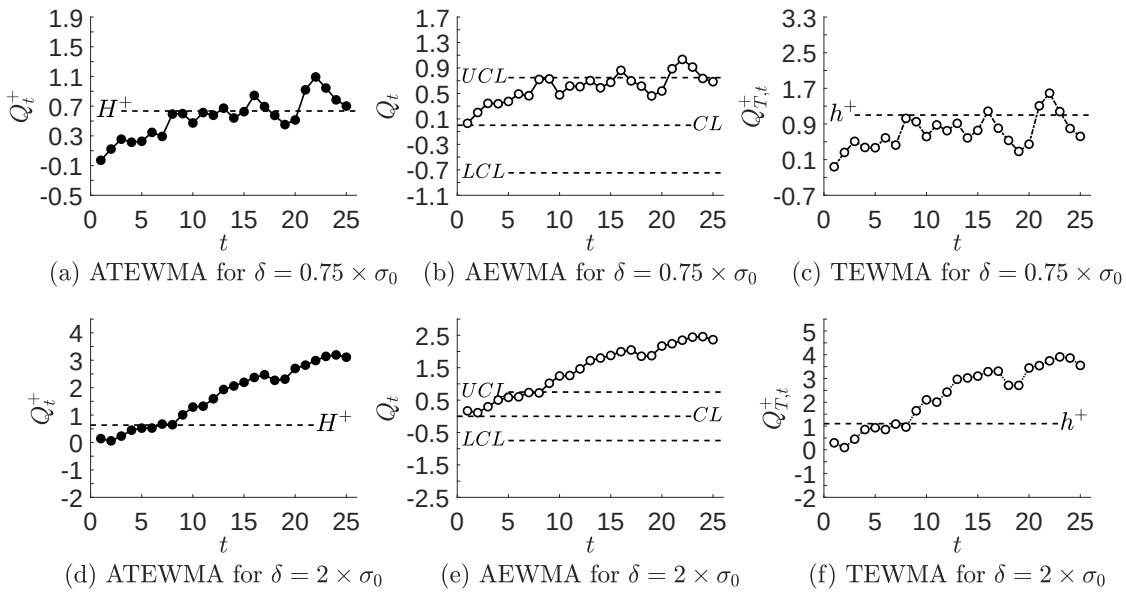

Figure 6: The recommended upper-sided ATEWMA $\bar{X}$ scheme, the conventional AEWMA $\bar{X}$ scheme, and the upper-sided TEWMA $\bar{X}$ scheme for monitoring zero-state datasets with $\delta = 0.75 \times \sigma_0$ and $\delta = 2 \times \sigma_0$, respectively.

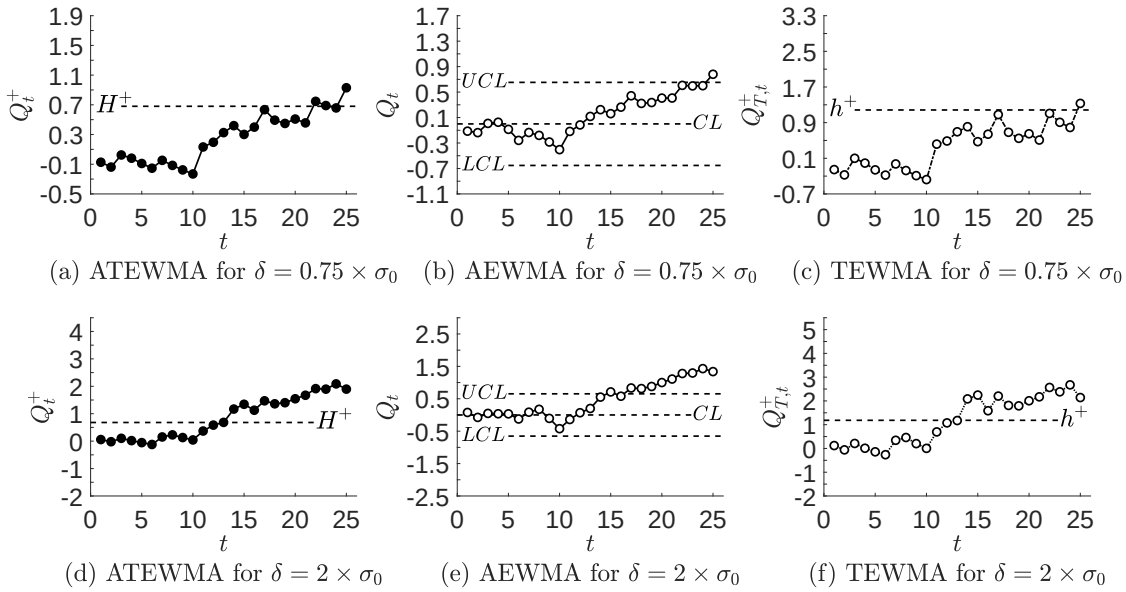

(a) ATEWMA for $\delta = 0.75 \times \sigma_0$ (b) AEWMA for $\delta = 0.75 \times \sigma_0$ (c) TEWMA for $\delta = 0.75 \times \sigma_0$

(d) ATEWMA for $\delta = 2 \times \sigma_0$ (e) AEWMA for $\delta = 2 \times \sigma_0$ (f) TEWMA for $\delta = 2 \times \sigma_0$

Figure 7: The recommended upper-sided ATEWMA $\bar{X}$ scheme, the conventional AEWMA $\bar{X}$ scheme, and the upper-sided TEWMA $\bar{X}$ scheme for monitoring steady-state datasets with $\delta = 0.75 \times \sigma_0$ and $\delta = 2 \times \sigma_0$, respectively.